Air particulate matter composition and sources at Westport

P K Davy W J Trompetter

GNS Science Consultancy Report 2024/04
January 2024 DRAFT

DISCLAIMER

This report has been prepared by the Institute of Geological and Nuclear Sciences Limited (GNS Science) exclusively for and under contract to West Coast Regional Council. Unless otherwise agreed in writing by GNS Science, GNS Science accepts no responsibility for any use of or reliance on any contents of this report by any person other than West Coast Regional Council and shall not be liable to any person other than West Coast Regional Council, on any ground, for any loss, damage or expense arising from such use or reliance.

Use of Data:

Date that GNS Science can use associated data: March 2024

BIBLIOGRAPHIC REFERENCE

Davy, P.K., Trompetter, W.J. 2024. Air particulate matter composition and sources at Westport. Lower Hutt (NZ): GNS Science. 57 p. Consultancy Report 2024/04.

CONTENTS

FIGURES

TABLES

APPENDICES

APPENDIX FIGURES

EXECUTIVE SUMMARY

This report presents the results of an analysis of particulate matter concentrations and composition from a winter $PM_{2.5}$ and PM_{10} sampling campaign at Westport on the west coast of the South Island. Particulate matter samples were collected from May 2023 to September 2023 as part of a $PM_{2.5}$ and PM_{10} airborne particle sampling programme at Westport. The sample set formed the basis of a study of particulate matter composition and the attribution of sources contributing to particulate matter concentrations. The particulate matter elemental composition data showed that black carbon, a product from combustion sources, was a dominant contributor to $PM_{2.5}$ concentrations. For PM_{10}, black carbon, sodium and chlorine were also important components which indicate the primary influence of the $PM_{2.5}$ combustion sources along with coarse particle marine aerosol (sea salt) sources.

Key results from the study are:

1. Four distinct source types were extracted from the data. These were: biomass combustion, motor vehicles, soil (crustal matter) and marine aerosol (sea salt).
2. The primary source of peak winter $PM_{2.5}$ in Westport was the biomass combustion source, which was attributed to the use of solid fuel fires for home heating and contributed 87% of the total $PM_{2.5}$ mass during peak concentrations (> than 15 µg m^{-3} the World Health Organisation ambient air quality guideline 24-hour average for $PM_{2.5}$).
3. Since the PM_{10} size fraction contains $PM_{2.5}$, contributions to peak PM_{10} concentrations reflected the influence of $PM_{2.5}$ combustion sources along with a greater influence of coarse particle sea salt and crustal matter.
4. The biomass combustion source associated with home heating emissions was found to be contaminated with arsenic and lead due to the opportunistic use of copper chrome arsenate-treated timber and old painted timber, respectively, as fuel.

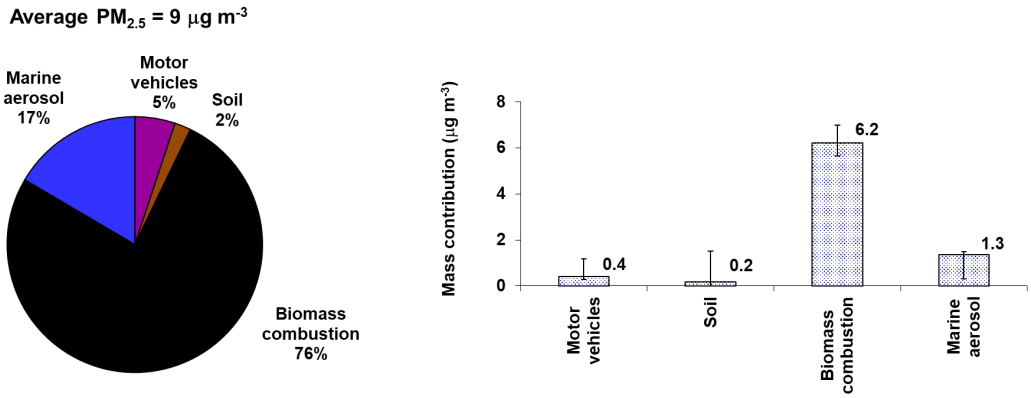

Figure ES1 Average source contributions to $PM_{2.5}$ at Westport over the monitoring period (May 2023 to September 2023).

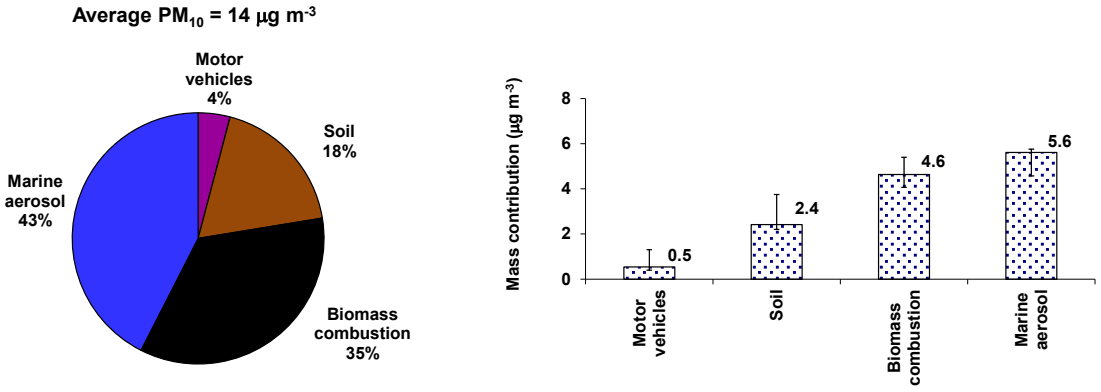

Figure ES2 Average source contributions to PM_{10} at Westport over the monitoring period (May 2023 to September 2023).

1.0 INTRODUCTION

This report presents the results of a compositional analysis and receptor modelling study of airborne particle samples collected during winter 2023 at an ambient air quality monitoring site in Westport. The work was commissioned by West Coast Regional Council (WCRC) as part of their ambient air quality monitoring programme and the requirement to manage air quality in the region. The work was partly funded by an Envirolink Grant (2405-WCRC211) from the Ministry of Business, Innovation and Employment.

1.1 Requirement to Manage Airborne Particle Pollution

In response to growing evidence of significant health effects associated with airborne particle pollution, the New Zealand Government introduced in 2004 a National Environmental Standard (NES) of 50 μg/m^3 for particles less than 10 μm in aerodynamic cross section (denoted as PM_{10}). The NES places the onus on regional councils to monitor PM_{10} and publicly report if the air quality in their region exceeds the standard with a provision for no more than one exceedance annually and a requirement for offsets by industry in PM_{10}-polluted airsheds replacing the restriction on industrial consents (Ministry for the Environment 2011).. Air pollution episodes that are outside regulatory authorities' ability to control may be considered 'exceptional events' by application for exemption (e.g. dust storms, volcanic eruptions)

In areas where the PM_{10} standard is exceeded, information on the sources contributing to those air pollution episodes is required to:

- identify 'exceptional events' outside of regulatory authority control;
- effectively manage air quality; and
- formulate appropriate mitigation strategies, where necessary.

In addition to the PM_{10} NES, the Ministry for the Environment issued ambient air quality guidelines (AAQGs) for air pollutants in 2002 that included a (monitoring) guideline value of 25 μg m^{-3} for $PM_{2.5}$ (24-hour average). More recently, the World Health Organisation (WHO) has confirmed a $PM_{2.5}$ ambient air quality guideline value of 15 μg m^{-3} (24-hour average) based on the relationship between 24-hour and annual PM levels (WHO 2021). The WHO annual average guideline for $PM_{2.5}$ is 5 μg m^{-3}. These are the lowest levels at which total, cardiopulmonary and lung cancer mortality have been shown to increase, with more than 95% confidence in response to exposure to $PM_{2.5}$. WHO recommends the use of $PM_{2.5}$ guidelines over PM_{10}, as epidemiological studies have shown that most of the adverse health effects associated with PM_{10} are due to $PM_{2.5}$. A recent analysis of the impact of air pollution on human health in New Zealand found that residential wood burning dominated the health effects associated with $PM_{2.5}$ pollution (Kuschel, Metcalfe et al. 2022).

1.1.1 Identifying Sources of Airborne Particulate Matter Pollution

Measuring the mass concentration of air particulate matter (PM) provides little information on the identity of the contributing sources. Airborne particles are composed of many elements and compounds from many different sources. Receptor modelling provides a means to determine the relative mass contribution of sources that impact significantly on the total mass of air particulate matter collected at a monitoring site. Elemental concentrations in PM filter samples were determined using X-ray fluorescence spectroscopy (XRF) at the New Zealand Ion Beam

Analysis Facility in Gracefield, Lower Hutt. Black carbon (BC) concentrations were determined using light reflectance techniques.

X-ray fluorescence spectroscopy is a mature analytical technique that provides a non-destructive determination of multi-elemental concentrations present in a sample. Using elemental concentrations with appropriate statistical techniques and purpose-designed mathematical models, the sources contributing to each ambient sample can be estimated. Appendix 1 provides a description of the XRF analytical process and receptor modelling techniques.

1.1.2 Scope of this Study

This report describes the sampling, results and outcomes according to the following objectives:

- Identify and quantify elemental concentrations in the PM samples including any toxic elements such as arsenic and lead;
- Identify and quantify those sources responsible for any exceedances of the NESAQ;
- Identify the sources of toxic emissions;
- Examine source contributions to PM with wind speed and direction;
- Identify and quantify the mass contribution to PM from sources that are difficult to quantify by emissions inventories or from natural sources that might fall outside the control of WCRC.

2.0 METHODOLOGY

2.1 Location of the Westport Particulate Matter Monitoring Site

Particulate matter ($PM_{2.5}$ and PM_{10}) sampling was undertaken by West Coast Regional Council (WCRC) from May 2023 until October 2023 at an air quality monitoring site at 44 Queen Street on the grounds of Club Buller, Westport (Lat -41.7511; Long 171.5998). The site is located in the middle of a mixed commercial/residential area as shown in Figure 2.1.

The authors have been provided with information about the monitoring site and have been informed of the typical activities in the surrounding areas that may contribute to PM concentrations. These details informed the conceptual receptor model described in Section 2.5.

Figure 2.1 Location of Westport monitoring site. (●) (image source: Google Earth 2023).

The area immediately around the site is flat and predominately residential, with local urban road traffic. Westport town centre and commercial area lies immediately to the west and southwest of the site with the Buller River beyond that. Further residential suburbs lie to the

north, east and south of the monitoring site. The coast (Buller Bay) is approximately 2 km directly north. Land-use surrounding the Westport urban area is predominantly agricultural.

2.2 Description of Particulate Matter Sampling at Westport

Particulate matter samples (24-hour time-integrated sampling period) for analysis were collected onto PTFE filters (TISCH PTFE membrane, 47mm 0.2µm) at the site using two MetOne sequential samplers (E-SEQ-FRM sequential reference method particulate sampler) located side-by-side. A total of 105 $PM_{2.5}$ and 81 PM_{10} samples (plus field blanks and lab blanks) were collected on a daily sampling regime over the monitoring period. All PM sampling and systems maintenance at the air quality monitoring site was carried out by WCRC, and as such, WCRC maintains all records of equipment, flow rates and sampling methodologies used for the PM sampling regime. Filter conditioning, weighing and re-weighing for PM gravimetric mass determinations were carried out by Hills Laboratories, Hamilton, in accordance with AS/NZS 3580.9.10 2006. Mass concentrations of PM were determined gravimetrically, where a filter of known weight was used to collect the PM samples from a known volume of sampled air. The loaded filters were then re-weighed to obtain the mass of collected PM. The average PM concentration in the volume of air sampled was then calculated.

2.3 Receptor Modelling Process

The multivariate analysis of air particulate matter sample composition (also known as receptor modelling) provides groupings (or factors) of elements that vary together over time. This technique effectively ‘fingerprints’ the sources that are contributing to airborne particulate matter and the mass of each element (and the PM mass) attributed to that source. In this study, the primary source contributors were determined using results from the Positive Matrix Factorisation (PMF analysis) of the particulate matter elemental composition.

A critical point for understanding the receptor modelling process is that the PMF model can produce any number of solutions, all of which may be mathematically correct (Paatero, Hopke et al. 2002). The “best” solution (e.g., number of factors, etc.) is generally determined by the practitioner after considering the model diagnostics and a review of the available factor profiles and contributions (to check physical interpretability). Most commonly used receptor models are based on conservation of mass from the point of emission to the point of sampling and measurement (Hopke 1999). Their mathematical formulations express ambient chemical concentrations as the sum of products of species abundances in source emissions and source contributions. In other words, the chemical profile measured at a monitoring station is resolved mathematically to be the sum of a number of different factors or sources. As with most modelling approaches, receptor models based on the conservation of mass are simplifications of reality and have the following general assumptions:

1. compositions of source emissions are constant over the period of ambient and source sampling;
2. chemical species do not react with each other (i.e., they add linearly);
3. all sources with a potential for contributing to the receptor have been identified and have had their emissions characterised;
4. the number of sources or source categories is less than or equal to the number of species measured;
5. the source profiles are linearly independent of each other; and
6. measurement uncertainties are random, uncorrelated, and normally distributed.

The effects of deviations from these assumptions are testable and can therefore allow the accuracy of source quantification to be evaluated. Uncertainties in input data can also be propagated to evaluate the uncertainty of source contribution estimates. There are a number of natural physical restraints that must be considered when developing a model for identifying and apportioning sources of airborne particles, these are (Hopke 2003):

- the model must explain the observations;
- the predicted source compositions must be non-negative;
- the predicted source contributions must be non-negative;
- the sum of predicted elemental mass contributions from each source must be less than or equal to measured mass for each element.

These constraints need to be kept in mind when conducting and interpreting any receptor modelling approach, particularly since a receptor model is still an approximation of the real-world system. Several factors also affect the nature of a source's particle composition and its contributions to ambient loadings (Brimblecombe 1986, Hopke 1999, Seinfeld and Pandis 2006):

1. the composition of particles emitted from a source may vary over time;
2. the composition of particles is modified in the atmosphere through a multitude of processes and interactions, for example;
    - adsorption of other species onto particle surfaces;
    - gas to particle conversions forming secondary particulate matter, for example the conversion of SO_2 gas to SO_4^{2-};
    - volatilisation of particle components such as organic compounds or volatilisation of Cl through reaction with acidic species;
    - interaction with, and transformation by, solar radiation and free radicals in the atmosphere such as the OH and NO_3 species.

The analytical processes used in this study did not analyse for nitrate (elemental hydrogen, carbon, oxygen and nitrogen are not detectable by XRF techniques), so the missing mass that the analysis is not explaining is likely a combination of nitrate and other unmeasured species such as hydrocarbons and bound water. Measurement of the ionic components in PM_{10} at other New Zealand sites indicates that aerosol nitrate species (primarily as $PM_{2.5}$) contributes approximately 0.25 μg m^{-3} in Auckland (Ancelet and Davy 2015) and 0.75 μg m^{-3} in Timaru (Scott 2014) to total PM mass during winter and somewhat less during other seasons due to atmospheric processing and thermodynamic equilibria (Seinfeld and Pandis 2006).

Analytical noise is also introduced during the species measurement process such as analyte interferences and limits of detection for species of interest. These are at least in the order of 5% for species well above its respective detection limit and 20% or more for those species near the analytical method detection limit (Hopke 1999). Further details on data analysis and dataset preparation are provided in Appendix 1.

2.4 Data Analysis and Reporting

The receptor modelling results within this report have been produced in a manner that provides as much information as possible on the relative contributions of sources to PM concentrations, so that it may be used for monitoring strategies, air quality management and policy development. The data have been analysed to provide the following outputs:

1. masses of elemental species apportioned to each source;
2. source elemental profiles;

3. average PM mass apportioned to each source;
4. temporal variations in source mass contributions (timeseries plots);
5. analysis of source contributions on peak PM days.

Table 2.1 presents the relevant standards, guidelines and targets for PM concentrations.

Table 2.1 Standards, guidelines and targets for PM concentrations.

Particle Size	Averaging Time	Ambient Air Quality Guideline (MfE 2002)	MfE* 'Acceptable' air quality category	MfE* 'Alert' air quality category	National Environmental Standard
PM_{10}	24 hours	50 µg m^{-3}	<33 µg m^{-3}	>33<50 µg m^{-3}	50 µg m^{-3}
	Annual	20 µg m^{-3}	<13 µg m^{-3}	>13<20 µg m^{-3}	
$PM_{2.5}$	24 hours	25 µg m^{-3}	<17 µg m^{-3}	>17<25 µg m^{-3}	

*Ministry for the Environment air quality categories taken from the Ministry for the Environment, October 1997 – ***Environmental Performance Indicators: Proposals for Air, Fresh Water and Land***.

2.4.1 Conditional Probability Function Analysis

A useful data analysis method is to investigate the relationship between the source contributions and wind direction. Bivariate polar plots using the source contributions to particulate matter were produced using R statistical software and the *openair* package (Team 2010, Carslaw 2012, Carslaw and Ropkins 2012). Using bivariate polar plots, source contributions can be shown as a function of both wind speed and direction, providing invaluable information about potential source regions and how pollution from a specific source builds up. To produce the polar plots, wind speeds and directions were vector averaged using functions available in *openair*. A full description of the vector averaging process can be found in Carslaw (2012).

Conditional Probability Function (CPF) analysis provides a method to find the directions for which high values of source contributions are likely to be related (Ashbaugh, Malm and Sadeh 1985). The probability that a source contribution originates from a given wind direction is estimated by comparing the wind direction distribution for the upper 25 % of source contributions relative to the total wind direction distribution.

$$CPF_{\Delta\theta} = \frac{m_{\Delta\theta}}{n_{\Delta\theta}}$$

Where:

$m_{\Delta\theta}$: Number of occurrences from wind sector $\Delta\theta$ for the upper 25% of source contributions.

$n_{\Delta\theta}$: Total number of occurrences from the same wind sector.

Sources are likely to be located in the directions that have high CPF values. Because of the smoothing involved, the colour scale is only to provide an indication of overall pattern and should not be interpreted in concentration units.

2.5 Conceptual Receptor Model for PM at Westport

An important part of the receptor modelling process is to formulate a conceptual model of the receptor site. This means understanding and identifying the major sources that may influence ambient PM concentrations at the site. For the Westport site, the initial conceptual model includes local emission sources:

- Domestic activities – likely to be dominated by biomass combustion activities such as emissions from solid fuel fires used for domestic heating during the winter;
- Motor vehicles – all roads in the area act as line sources, and roads with higher traffic densities will dominate emissions;
- Industrial emissions from combustion processes (boilers) and dust generating activities such as excavation, construction and bulk storage handling;
- Local wind-blown soil or road dust sources may also contribute.

Sources that originate further from the monitoring site would also be expected to contribute to ambient particle loadings. These include:

- Marine aerosol (sea salt) generated in the oceanic regions around New Zealand;
- Secondary PM resulting from atmospheric gas-to-particle conversion processes – includes sulphates, nitrates and organic species.

Another category of emission sources that may contribute are those considered to be ‘one-off’ emission sources:

- Fireworks displays and other special events (e.g. Guy Fawkes Day);
- Short-term road works and demolition/construction activities.

The variety of sources described above can be recognised and accounted for using appropriate data analysis methods, such as the application of geochemical principles, examination of seasonal differences, temporal variations, and receptor modelling itself.

2.6 Local Meteorology at Westport

Meteorological data was obtained from an automatic weather station, (Westport EWS; Network number F11765; Lat -41.743; Long 171.612; operated by NIWA Ltd) located approximately 2 km northeast of the monitoring site. As shown in Figure 2.2, the predominant wind directions were from the southwest quadrant for the monitoring period (May 2023 – September 2023).

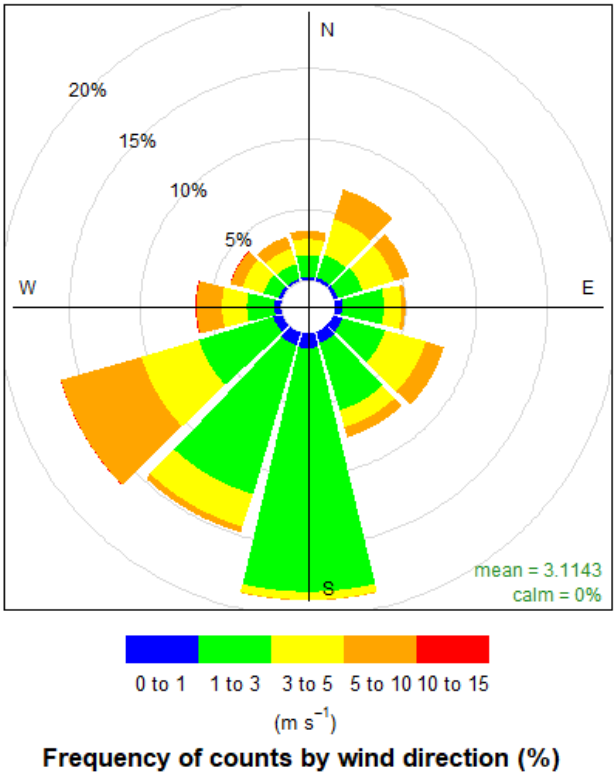

Figure 2.2 Wind rose for the monitoring period at Westport. (May 2023 – September 2023).

2.7 $PM_{2.5}$ and PM_{10} Concentrations at Westport

Mass concentrations were determined gravimetrically by Hills Laboratories Ltd for the Westport $PM_{2.5}$ and PM_{10} sample filters. Figures 2.3 and 2.4 present the $PM_{2.5}$ and PM_{10} monitoring results (24-hour averages, midnight to midnight sampling regime) over the monitoring period (May 2023 – September 2023). Gaps present in Figures 2.3 and 2.4 are from sampler outages and/or maintenance. The WHO ambient air quality guideline (WHO AAQG) concentration (15 µg m^{-3} as a 24-hour average) for $PM_{2.5}$ was exceeded on 6 occasions during the monitoring period. The National Environment Standard Air Quality Standard (NESAQ) for PM_{10} (50 µg m^{-3} as a 24-hour average) was not exceeded during the filter sampling campaign.

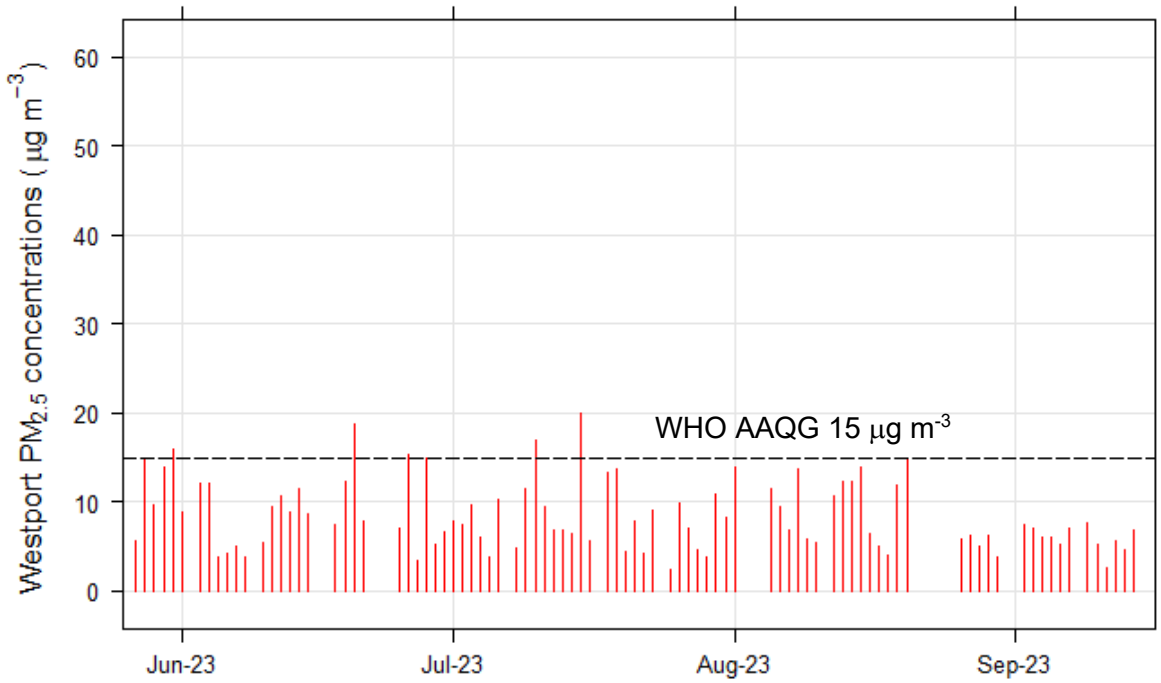

Figure 2.3 Gravimetric $PM_{2.5}$ (24-hour average) concentrations at Westport. Note that the gaps in the graph are due to missing samples. The dashed line indicates the WHO ambient air quality guideline (WHO AAQG) concentration (15 µg m^{-3} as a 24-hour average) for $PM_{2.5}$.

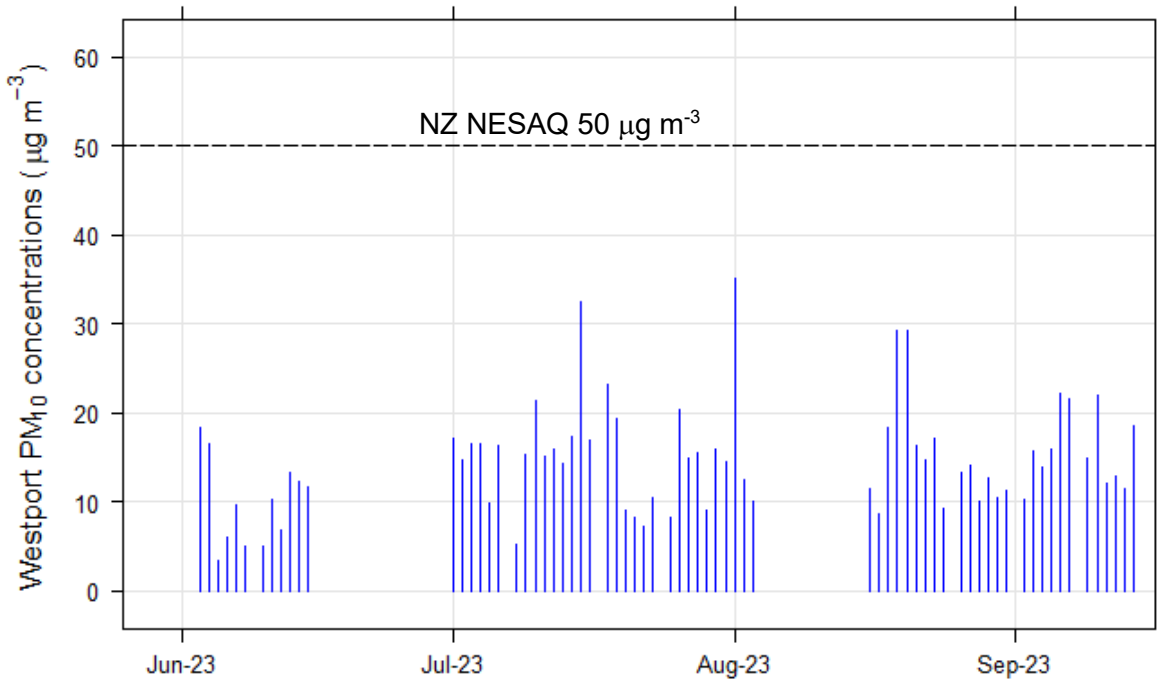

Figure 2.4 Gravimetric PM_{10} (24-hour average) concentrations at Westport. Note that the gaps in the graph are due to missing samples. The dashed line indicates the National Environment Standard Air Quality Standard (NESAQ) for PM_{10} (50 µg m^{-3} as a 24-hour average).

3.0 RECEPTOR MODELLING ANALYSIS OF WESTPORT PARTICULATE MATTER SOURCES

3.1 Analysis of Particulate Matter Samples Collected at Westport

$PM_{2.5}$ and PM_{10} samples at Westport were collected by WCRC using a MetOne sequential sampler system on a daily sampling regime over the monitoring period. Overall, a total of 103 $PM_{2.5}$ and 81 PM_{10} samples (plus field blanks and lab blanks) were collected from May 2023 to September 2023. Elemental and black carbon (BC) concentrations in the particulate matter samples were determined using XRF and light reflection respectively, as described in Appendix 1.

3.1.1 Composition of $PM_{2.5}$ at Westport

Elemental concentrations in the $PM_{2.5}$ samples collected at the Westport monitoring site are presented in Table 3.1. Note that it was found that the filters used for the Westport sampling campaign had a high background of silicon on the field blank and lab blanks. This precluded any sensible data for silicon and aluminium (aluminium has an X-ray energy peak immediately adjacent silicon) after blank subtraction. Silicon and aluminium (along with Ca, Ti and Fe) are key components of crustal matter (soil) which is usually one of the main sources contributing to ambient particulate matter at urban locations, particularly to the coarse ($PM_{10-2.5}$) fraction. The data show that $PM_{2.5}$ concentrations were dominated by BC during the winter months. Other important elemental constituents included K, Na, Cl, S, and Fe, indicating that combustion sources, marine aerosol, and crustal matter were likely to be important contributors to $PM_{2.5}$ concentrations at the monitoring site. Some measured species were close to or below their respective limit of detection (LOD) in each of the samples. Appendix 1 provides a description of data treatment and detection limits. Elemental correlation plots are provided in Figure A2.2 in Appendix 2.

Table 3.1 Elemental concentrations in $PM_{2.5}$ samples from Westport (103 samples).

	Unit	Average	Maximum	Minimum	Median	Std Dev	Average LOD	% > LOD
$PM_{2.5}$	µg m^{-3}	9	21	2	8	6		
BC	ng m^{-3}	3119	6919	208	2837	1378	115	100
Na	ng m^{-3}	538	1903	38	417	693	5	100
Mg	ng m^{-3}	50	179	0	38	91	10	82
P	ng m^{-3}	0	0	0	0	0	2	0
S	ng m^{-3}	143	430	29	124	114	0	100
Cl	ng m^{-3}	614	2645	9	365	1544	1	100
K	ng m^{-3}	84	194	33	70	46	9	100
Ca	ng m^{-3}	11	48	0	6	45	1	74
Ti	ng m^{-3}	1	5	0	1	10	1	34
V	ng m^{-3}	0	2	0	0	0	0	20
Cr	ng m^{-3}	0	1	0	0	0	2	0

Mn	ng m^{-3}	1	7	0	1	2	2	21
Fe	ng m^{-3}	8	43	0	7	29	2	85
Co	ng m^{-3}	0	1	0	0	0	0	15
Ni	ng m^{-3}	79	2133	0	0	297	1	22
Cu	ng m^{-3}	1	7	0	0	1	2	23
Zn	ng m^{-3}	5	35	0	4	5	1	93
Ga	ng m^{-3}	0	4	0	0	1	1	19
As	ng m^{-3}	7	55	0	2	11	1	58
Se	ng m^{-3}	0	3	0	0	1	1	10
Br	ng m^{-3}	2	7	0	2	6	1	67
Sr	ng m^{-3}	1	10	0	0	2	1	37
Mo	ng m^{-3}	12	1176	0	0	87	2	27
Cd	ng m^{-3}	10	61	0	1	13	21	20
Sn	ng m^{-3}	4	23	0	1	6	10	17
Sb	ng m^{-3}	5	28	0	2	7	11	22
Te	ng m^{-3}	6	46	0	1	9	13	17
Cs	ng m^{-3}	7	35	0	3	9	15	19
Ba	ng m^{-3}	7	58	0	2	11	15	19
La	ng m^{-3}	11	80	0	3	15	22	24
Ce	ng m^{-3}	47	483	0	0	93	123	16
Sm	ng m^{-3}	35	247	0	0	60	85	16
Pb	ng m^{-3}	6	18	0	5	5	3	72
Hg	ng m^{-3}	1	12	0	0	2	2	23
In	ng m^{-3}	2	13	0	0	3	5	14
W	ng m^{-3}	70	399	0	3	98	151	18

3.1.2 Composition of PM_{10} at Westport

Elemental concentrations in the PM_{10} samples collected at the Westport monitoring site are presented in Table 3.2. Since PM_{10} contains the $PM_{2.5}$ fraction, the data show that PM_{10} BC concentrations were similar to $PM_{2.5}$. However, elemental constituents such as, Na, Cl, S, Ti and Fe were significantly higher in PM_{10}, indicating that coarse particle ($PM_{10-2.5}$ fraction) sources, such as marine aerosol and crustal matter, were likely to be important contributors to PM_{10} concentrations at the monitoring site in addition to the $PM_{2.5}$ sources described in Section 3.1.1.

Table 3.2 Elemental concentrations in PM_{10} samples from Westport (81 samples).

	Unit	Average	Maximum	Minimum	Median	Std Dev	Average LOD	% > LOD
$PM_{2.5}$	µg m^{-3}	14	35	3	14	6		
BC	ng m^{-3}	2711	6456	387	2528	1378	110	99
Na	ng m^{-3}	1223	3413	62	1177	693	5	99
Mg	ng m^{-3}	155	492	0	141	91	10	96
P	ng m^{-3}	0	0	0	0	0	1	0
S	ng m^{-3}	241	692	63	237	114	0	99
Cl	ng m^{-3}	2416	6966	38	2119	1544	1	99
K	ng m^{-3}	126	293	43	120	46	9	99
Ca	ng m^{-3}	74	261	7	67	45	1	99
Ti	ng m^{-3}	6	97	0	2	10	1	75
V	ng m^{-3}	0	3	0	0	0	0	29
Cr	ng m^{-3}	0	2	0	0	0	2	4
Mn	ng m^{-3}	2	11	0	1	2	2	40
Fe	ng m^{-3}	42	196	4	33	29	2	99
Co	ng m^{-3}	0	1	0	0	0	0	14
Ni	ng m^{-3}	0	2	0	0	297	1	18
Cu	ng m^{-3}	1	8	0	1	1	1	43
Zn	ng m^{-3}	7	37	0	6	5	1	96
Ga	ng m^{-3}	0	3	0	0	1	1	25
As	ng m^{-3}	7	57	0	4	11	1	59
Se	ng m^{-3}	0	2	0	0	1	1	9
Br	ng m^{-3}	9	37	0	7	6	1	88
Sr	ng m^{-3}	2	6	0	1	2	1	48
Mo	ng m^{-3}	1	5	0	0	87	2	21
Cd	ng m^{-3}	13	48	0	10	13	20	33
Sn	ng m^{-3}	6	29	0	4	6	9	25
Sb	ng m^{-3}	7	30	0	5	7	10	33
Te	ng m^{-3}	8	37	0	6	9	13	30
Cs	ng m^{-3}	8	43	0	5	9	14	26

Ba	ng m^{-3}	10	47	0	6	11	14	31
La	ng m^{-3}	12	61	0	5	15	21	28
Ce	ng m^{-3}	50	771	0	0	93	117	15
Sm	ng m^{-3}	43	281	0	6	60	81	21
Pb	ng m^{-3}	6	22	0	6	5	2	80
Hg	ng m^{-3}	1	6	0	0	2	2	13
In	ng m^{-3}	3	28	0	1	3	5	21
W	ng m^{-3}	89	426	0	46	98	144	30

Note that due to instrument outages at different times for $PM_{2.5}$ and PM_{10} sampling (see Figures 2.3 and 2.4) the statistics presented in Tables 3.1 and 3.2 are not necessarily comparable. However, the simultaneous monitoring of the two size fractions provides the opportunity to directly compare component species for those samples that were coincident. For example, black carbon concentrations in both $PM_{2.5}$ and PM_{10} were found to be essentially the same (slight differences are due to sampling and measurement uncertainty), as presented in Figure 3.1. This is because black carbon particles, a product of incomplete combustion, are all smaller than 2.5 microns and are therefore entirely contained in the $PM_{2.5}$ fraction (a subset of PM_{10}).

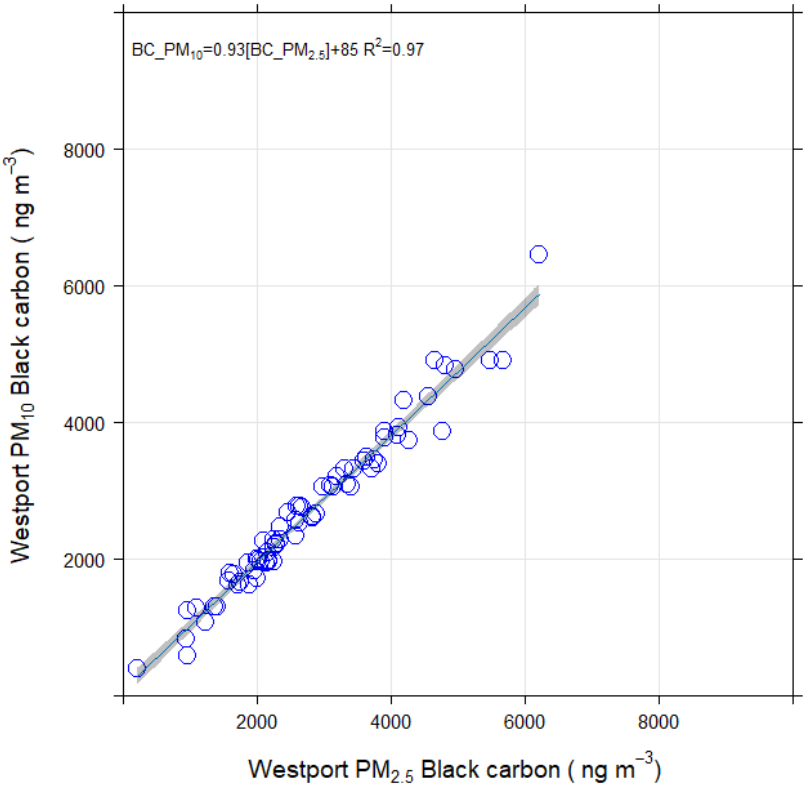

Figure 3.1 Black carbon concentrations in $PM_{2.5}$ versus PM_{10} samples from Westport.

Of the measured heavy metals, arsenic was found to have similar concentrations in $PM_{2.5}$ and PM_{10}, as presented in Figure 3.2, indicating that the metal was derived from a fine particle emission source.

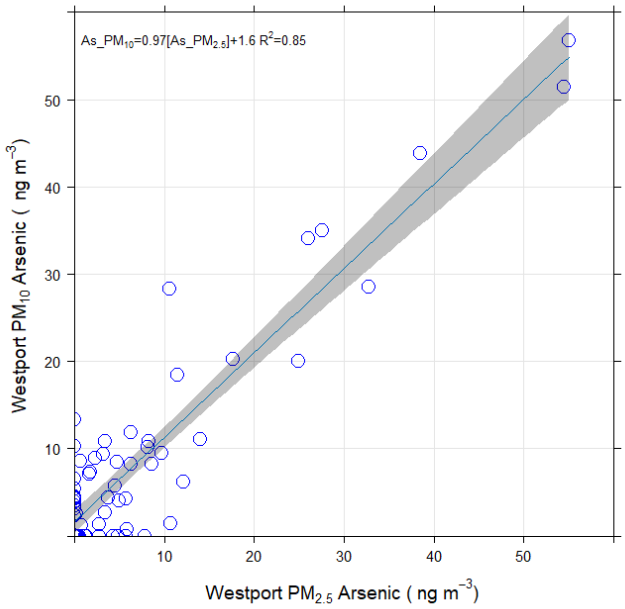

Figure 3.2 Arsenic concentrations in $PM_{2.5}$ versus PM_{10} samples from Westport.

Inhalation of such contaminated air particulate matter has been shown to result in biological uptake in humans with the long-term effects of exposure as yet unknown (Dirks, Chester et al. 2020).

3.2 Source Contributions to Particulate Matter at Westport

The $PM_{2.5}$ and PM_{10} compositional data were analysed to provide information on contributing sources using PMF with multiple reiterations such that robust solutions and source attributions were arrived at. Sources of PM emissions or generation include particles across the size-range spectrum and therefore contribute to both fine and coarse size fractions, although some source types will contribute more to one size fraction than the other. For example, combustion sources, such as domestic solid fuel fires or motor vehicle tailpipe emissions, produce particles in the sub-micron size range and are therefore largely confined to the $PM_{2.5}$ fraction. Windblown dust, non-exhaust emissions (NEE) generated from brakes, tyres and by the turbulent passage of vehicles over local roads, sea salt or industrial processes that involve mechanical grinding, sorting, storage and transport of bulk materials, predominantly produce particles in the larger size ranges (> $PM_{2.5}$) although some 'tail' of particle sizes does extend down into the $PM_{2.5}$ size fraction.

3.2.1 Sources of $PM_{2.5}$ and PM_{10} at Westport

Four source types were identified from PMF receptor modelling analysis of the Westport $PM_{2.5}$ and PM_{10} elemental data. The source contributors identified were found to explain 98% of the $PM_{2.5}$ and 90% of the PM_{10} mass on average.

The sources identified were:

- **Biomass combustion**: The first factor was identified as biomass combustion based on the dominance of BC and K in the profile (Fine, Cass and Simoneit 2001, Khalil and Rasmussen 2003). Trace amounts of arsenic and lead were also strongly associated with the biomass combustion profile. This phenomenon is consistent throughout New Zealand and indicates co-combustion of copper chrome arsenate-treated (CCA) timber and old painted timber respectively (Davy, Ancelet et al. 2014);
- **Motor vehicles**: The second factor was identified as motor vehicles because of the presence of BC, Fe, Cu and Zn as significant elemental components. This profile is likely a combination of tailpipe (BC and Zn from fuel combustion) and re-entrained road dust emissions (Ca, Ti, Fe from crustal matter components, Cu from brake dust, Zn from tyre wear).
- **Soil**: a third source was identified as originating from activities that generate emissions of crustal matter to atmosphere. Crustal matter is primarily composed of aluminosilicate minerals and the source profiles extracted from receptor modelling usually reflect this. However, without Si or Al available in this analysis, other mineral constituents such as Mg, K, Ca, Ti and Fe have provided the basis of identifying this source. Crustal matter (synonymous with 'soil' as a source reference) is predominantly a coarse particle source generated by mechanical abrasion of surface material. At urban locations, the passage of motor vehicles over roads can be the primary source of crustal matter suspension and resuspension (Davy and Trompetter 2021, Thorpe and Harrison, 2008).
- **Marine aerosol**: The fourth factor was identified as a marine aerosol source because of the predominance of Na and Cl, along with some Mg, S, K, and Ca in similar ratios to sea water.

Figure 3.3 presents the source elemental profiles for the $PM_{2.5}$ and PM_{10} source contributors.

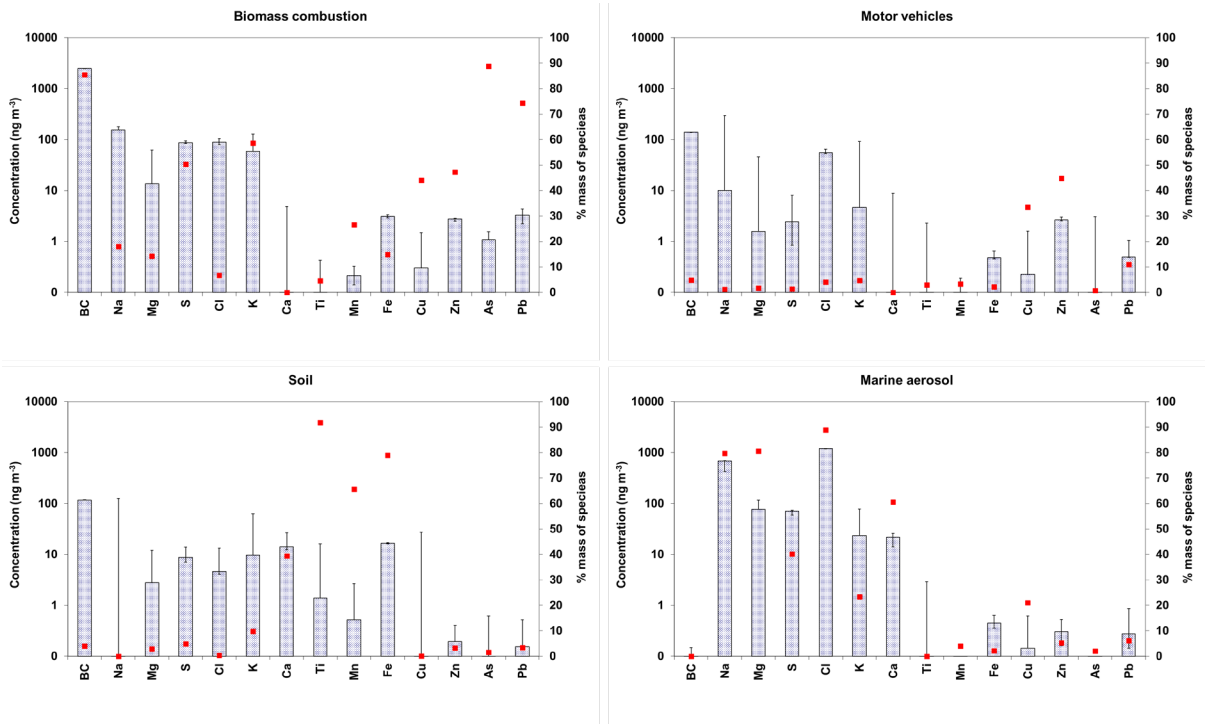

Figure 3.3 Source elemental concentration profiles for particulate matter samples from Westport The red dots represent the percentage of each chemical species attributed to each source.

Table 3.3 presents the average source elemental concentration profiles for $PM_{2.5}$ samples derived from the PMF analysis.

Table 3.3 Average source elemental concentration profiles for $PM_{2.5}$ samples from Westport (based on 103 samples).

	Biomass combustion (ng m^{-3})	Motor vehicles (ng m^{-3})	Soil (ng m^{-3})	Marine aerosol (ng m^{-3})
$PM_{2.5}$	6220	420	168	1350
BC	2575.1	146.7	70.96	284.1
Na	137.9	2.3	5.73	394.9
Mg	12.3	0.4	0.0	37.3
S	86.0	2.6	6.1	37.6
Cl	79.9	18.7	0.0	511.3
K	59.2	4.1	3.2	15.5
Ca	0.0	0.0	4.4	6.1
Ti	0.2	0.0	0.2	0.0
Mn	0.3	0.1	0.1	0.0
Fe	3.9	0.3	1.8	0.0
Cu	0.1	0.1	0.0	0.1
Zn	2.9	1.9	0.2	0.2
As	1.1	0.0	0.0	0.1
Pb	3.9	0.4	0.0	0.5

Table 3.3 shows that biomass combustion was the dominant contributing source to average $PM_{2.5}$ concentrations at Westport during the monitoring period. Note that the summation of elemental components does not equal PM mass, as this analysis was not for compounds (which includes oxides and other unmeasured species as described in Section 2.1), but for proportional elemental covariance and the proportion of particulate matter mass that is also covariant with those elemental species.

Figure 3.4 presents the relative source contributions to $PM_{2.5}$ in Westport. Also included in Figure 3.4 are the 5^{th} and 95^{th} percentile confidence limits (bottom and top of error bar respectively) in average mass contributions attributed to each of the sources, indicating the variability in average mass contributions over the monitoring period.

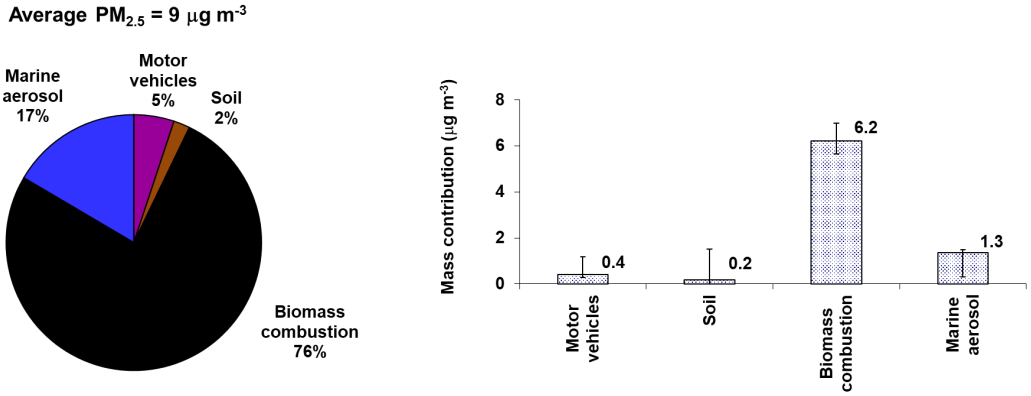

Figure 3.4 Average source mass contributions to $PM_{2.5}$ at Westport over the monitoring period.

The average $PM_{2.5}$ source contributions over the monitoring period estimated from the PMF analysis showed that biomass combustion (76%) was the most significant contributor to $PM_{2.5}$ mass with marine aerosol (17%) and motor vehicles (5%) the next highest, while soil (2%) had the lowest contributions to $PM_{2.5}$ mass.

Table 3.4 presents the average source elemental concentration profiles for PM_{10} samples derived from the PMF analysis.

Table 3.4 Average source elemental concentration profiles for PM_{10} samples from Westport (based on 81 samples).

	Biomass combustion (ng m^{-3})	Motor vehicles (ng m^{-3})	Soil (ng m^{-3})	Marine aerosol (ng m^{-3})
PM_{10}	4630	541	2420	5610
BC	2215.7	324.4	154.6	0
Na	102.1	115.4	14.7	994.3
Mg	17.1	11.9	2.8	120.6
S	96.8	10.9	5.6	116.2
Cl	56.2	252.9	0.0	2076.0
K	62.0	13.2	10.3	38.6
Ca	11.0	3.7	12.7	43.0
Ti	0.0	0.0	3.7	0.2
Mn	0.1	0.0	0.9	0.2
Fe	15.1	0.0	26.1	0.0
Cu	0.4	0.6	0.0	0.0
Zn	4.0	2.2	0.4	0.2
As	1.2	0.0	0.0	0.0

Pb	2.9	0.2	1.2	0.2

Table 3.4 also shows that marine aerosol (sea salt) and biomass combustion were the dominant contributing sources to average PM_{10} concentrations at Westport.

Figure 3.5 presents the relative source contributions to PM_{10} in Westport. Also included in Figure 3.5 are the 5th and 95th percentile confidence limits (bottom and top of error bar respectively) in average mass contributions attributed to each of the sources, indicating the variability in average mass contributions over the monitoring period.

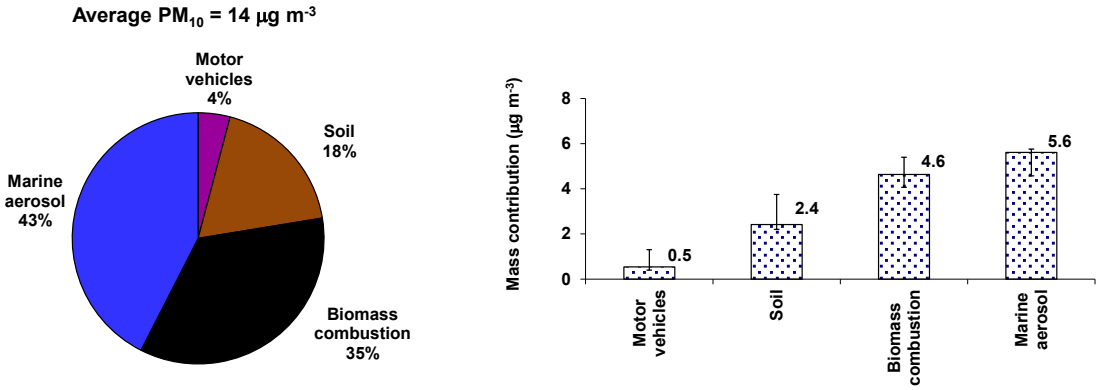

Figure 3.5 Average source mass contributions to PM_{10} at Westport over the monitoring period.

The average PM_{10} source contributions over the monitoring period estimated from the PMF analysis showed that marine aerosol (43%) was the most significant contributor to PM_{10} mass with biomass combustion (35%) with soil (18%) the next highest, while motor vehicles (4%) had the lowest contributions to PM_{10} mass.

3.3 Temporal Variations in Source Contributions to Particulate Matter at Westport

Temporal variations in the source contributions to $PM_{2.5}$ and PM_{10} at Westport are presented in Figure 3.6 and Figure 3.7, respectively. It was evident from the data that $PM_{2.5}$ mass is dominated by the biomass combustion source during winter, which arises primarily from emissions from solid fuel fires used for domestic heating. It is also evident that significantly more marine aerosol and crustal matter particles are present in PM_{10} indicating the coarse particle nature of those sources. The motor vehicle source contributed low levels of $PM_{2.5}$ during the monitoring period, most likely due to the local level of traffic activity nearby the Westport monitoring site. However, motor vehicles may also be the predominant source of resuspended crustal matter as non-exhaust emissions in urban locations.

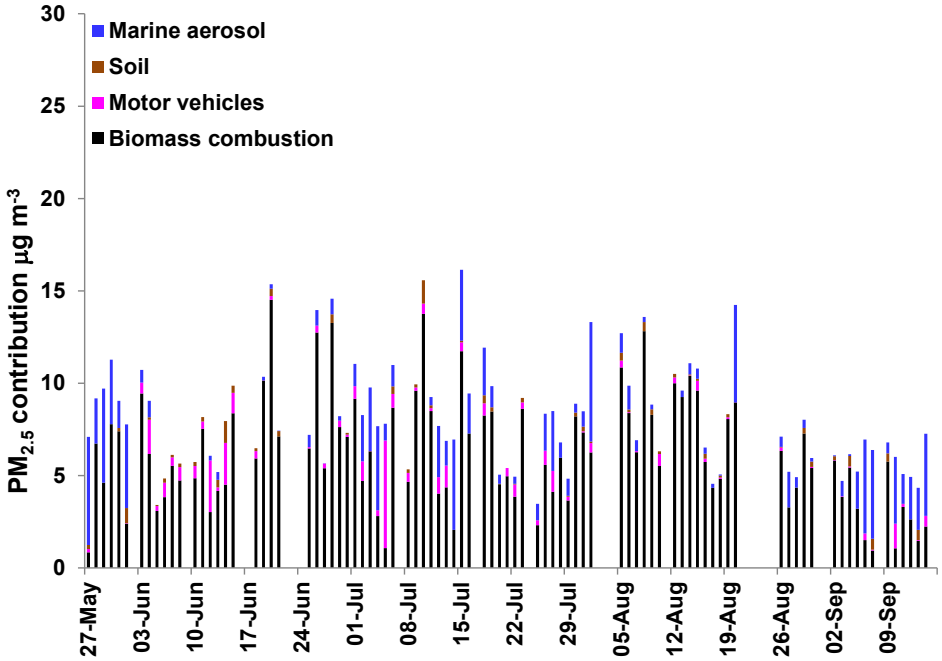

Figure 3.6 Temporal variations in relative source contributions to $PM_{2.5}$ mass (24-hour average) at the Westport site.

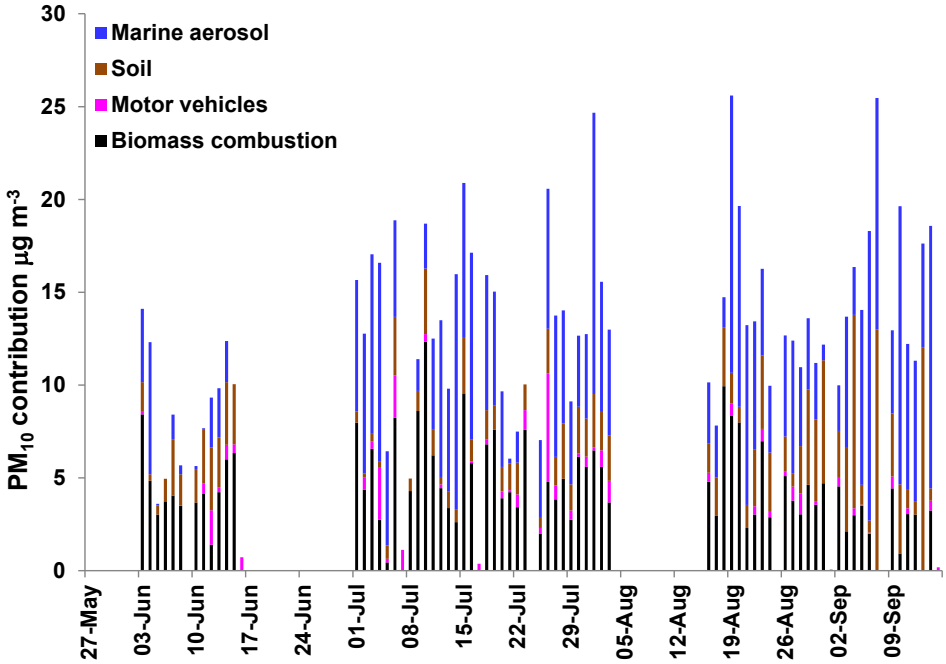

Figure 3.7 Temporal variations in relative source contributions to PM_{10} mass (24-hour average) at the Westport site.

3.4 Variations in Source Contributions at Westport with Wind Direction

Bivariate polar plots using the source contributions to $PM_{2.5}$ were produced using R statistical software and the *openair* package (Team 2010, Carslaw 2012, Carslaw and Ropkins 2012). Using bivariate polar plots, source contributions can be shown as a function of both wind speed and direction, providing invaluable information about potential source regions and how pollution from a specific source builds up. To produce the polar plots, wind speeds and directions were vector averaged using functions available in *openair*. A full description of the vector averaging process can be found in Carslaw (2012). The conditional probability function statistic = "cpf" has been used here as described in Section 2.2.1. Because of the smoothing involved, the colour scale used in the plots is only to provide an indication of overall pattern and should not be interpreted in concentration units. The meteorological data used for the polar plot analysis was that supplied by WCRC from the Westport EWS operated by NIWA Ltd (see Section 2.6).

3.4.1 Biomass Combustion

Biomass combustion source contributions to $PM_{2.5}$ and PM_{10} were considered to be primarily from domestic solid fuel fire emissions. Figure 3.8 presents a bivariate polar plot of biomass combustion contributions to particulate matter at the monitoring site. Figure 3.8 shows that peak biomass combustion contributions occurred under light winds (less than 2 m/s) from the southeast. This suggests that light winds, most likely katabatic drainage flows under calm meteorological conditions, coupled with domestic fire emissions and poor dispersion, were responsible for elevated particulate matter concentrations. Similar meteorological conditions along with domestic solid fuel heating emissions into an airshed have been observed to lead elevated particulate matter concentrations at other New Zealand locations (Trompetter, Davy and Markwitz 2010, Ancelet, Davy et al. 2012, Grange, Salmond et al. 2013, Ancelet, Davy et al. 2014).

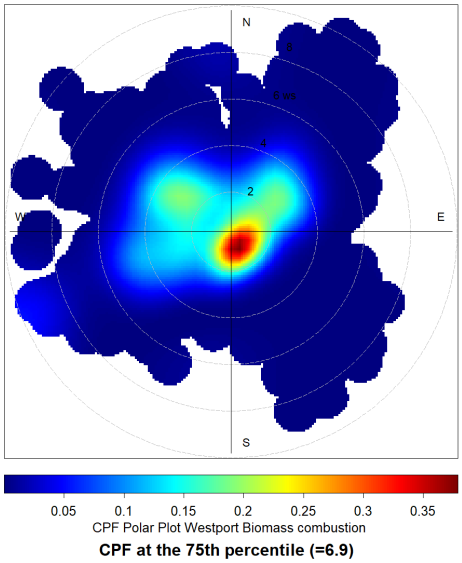

Figure 3.8 Polar plot of biomass combustion contributions to $PM_{2.5}$ and PM_{10} concentrations. The radial dimensions indicate the wind speed in 2 m s^{-1} increments and the colour contours indicate the relative contribution to each wind direction/speed bin. Because of the smoothing involved, the colour scale used in the plots is only to provide an indication of overall pattern and should not be interpreted in concentration units.

3.4.2 Motor Vehicles

Peak motor vehicle contributions at the monitoring site occurred under winds from the southwest quadrant (Figure 3.9). This is likely to represent the contribution from motor vehicles on the local roading network and activity in the commercial centre to the southwest of the monitoring site. When wind direction aligns with the centreline of roadways, the road acts as a line source and this will convey the highest concentrations of motor vehicle emissions.

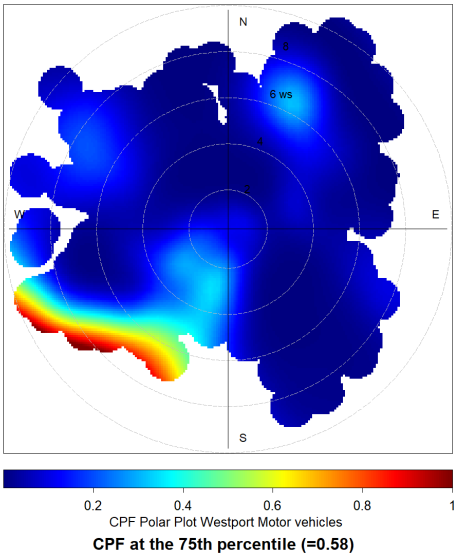

Figure 3.9 Polar plot of motor vehicle contributions to $PM_{2.5}$ and PM_{10} concentrations. The radial dimensions indicate the wind speed in 2 m s^{-1} increments and the colour contours indicate the relative contribution to each wind direction/speed bin. Because of the smoothing involved, the colour scale used in the plots is only to provide an indication of overall pattern and should not be interpreted in concentration units.

3.4.3 Soil

Figure 3.10 shows that the crustal matter contributions peaked under light wind speeds from the south. The crustal matter in urban areas is likely to be generated by a combination of vehicle dusts from road surfaces, unsealed yards or other dust generating activities. In addition, agricultural activities, land excavations, and the processing, handling or storage of bulk aggregate may also be potential sources.

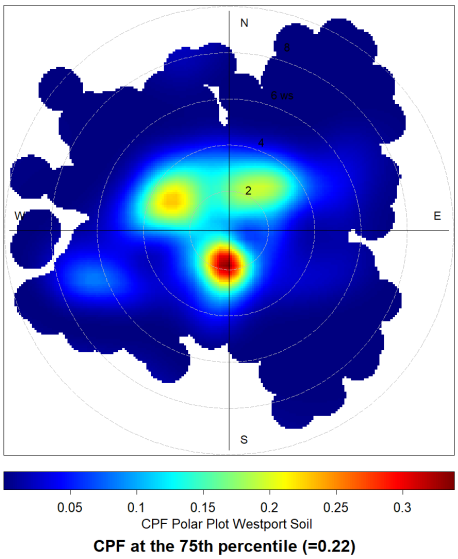

Figure 3.10 Polar plot of Soil contributions to $PM_{2.5}$ and PM_{10} concentrations. The radial dimensions indicate the wind speed in 2 m s^{-1} increments and the colour contours indicate the relative contribution to each wind direction/speed bin. Because of the smoothing involved, the colour scale used in the plots is only to provide an indication of overall pattern and should not be interpreted in concentration units.

3.4.4 Marine Aerosol

Marine aerosol contributions in Westport peaked under higher wind speeds from the northerly and southwesterly sectors which aligns with significant oceanic wind fetch (Figure 3.11). The marine aerosol (sea salt) source concentrations were likely to be primarily a meteorologically generated source (wind field strength over oceanic fetch) (Fitzgerald 1991). The most likely source of marine aerosol was the Tasman Sea and Southern Ocean.

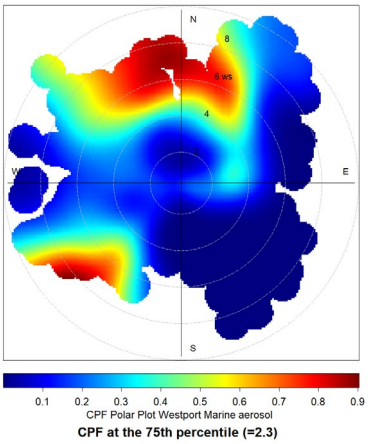

Figure 3.11 Polar plot of marine aerosol contributions to $PM_{2.5}$ and PM_{10} concentrations. The radial dimensions indicate the wind speed in 2 m s^{-1} increments and the colour contours indicate the relative contribution to each wind direction/speed bin. Because of the smoothing involved, the colour scale used in the plots is only to provide an indication of overall pattern and should not be interpreted in concentration units.

4.0 DISCUSSION OF THE WESTPORT RECEPTOR MODELLING RESULTS

Four primary source contributors to $PM_{2.5}$ and PM_{10} concentrations at Westport were identified from receptor modelling of particulate matter sample composition, The simultaneous collection of $PM_{2.5}$ and PM_{10} at the Westport monitoring site has provided the means to intercompare source contributions to each size fraction and examine any differences. The receptor modelling analysis showed that peak winter $PM_{2.5}$ concentrations were primarily influenced by biomass combustion sources, while marine aerosol and biomass combustion dominated PM_{10} concentrations.

4.1 Sources of Particulate Matter at Westport

4.1.1 Biomass Combustion

The biomass combustion source was most likely to have originated from domestic wood combustion for home heating and included traces of arsenic and lead in the source chemical profile, suggesting that CCA-treated wood and old painted timber were being used as fuel. The use of such contaminated timber as fuel for domestic fires appears to be common throughout New Zealand (Davy, Ancelet et al. 2012, Ancelet, Davy and Trompetter 2013, Mitchell, Davy et al. 2013, Ancelet, Davy and Trompetter 2014, Ancelet, Davy et al. 2014, Davy, Ancelet et al. 2014, Davy, Ancelet and Trompetter 2016, Davy and Trompetter 2017, Davy and Trompetter 2017, Davy and Trompetter 2018, Davy and Trompetter 2019). While coal may also be used as fuel in domestic heating appliances, the source chemical profile (see Figure 3.3) suggests that wood is the dominant fuel. In any case, due to the covariant nature of both wood and coal emissions from domestic fires, it would be difficult to separate source contributions from the different fuels over a short study period.

An interesting feature of the Westport elemental data were the concentrations of arsenic in both $PM_{2.5}$ and PM_{10}. Figure 3.2 shows that concentrations of the heavy metal was correlated between the two size fractions, and the receptor modelling showed that As along with Pb were associated with emissions of biomass combustion particles. However, when As and Pb concentrations were compared to each other and the biomass combustion source contributions, it was found that there was much more scatter. It is likely that, rather than being used as a constant percentage of solid fuels, contaminated timber use is more opportunistic and probably only by certain households in the area. There were occasions where arsenic or lead were not detected even though biomass combustion contributions were present. Similar results were observed for a recently completed analysis of $PM_{2.5}$ composition and sources at Motueka in the Tasman District (Davy, and Trompetter. 2023) and for $PM_{2.5}$ and PM_{10} at Hastings in the Hawke's Bay Region (Davy and Trompetter 2024).

4.1.2 Motor vehicles

The motor vehicle source was identified as a minor contributor to $PM_{2.5}$ (5 %) and PM_{10} (4%) at Westport. As indicated in the previous sections, the motor vehicle source is likely to be a combination of vehicular tailpipe emissions (fine particles) and re-suspended material (coarse particles) including crustal matter, brake wear and tyre wear generated by the turbulent passage of vehicles on roads, carparking areas and unsealed yards. At other urban locations in New Zealand, the motor vehicle and soil sources have been found to be associated. The evidence for this based on a weekday/weekend difference in source contributions for both source types (Davy and Trompetter 2021). A similar statistical temporal variation analysis was not possible for the Westport data due to the short (winter only) duration of the sampling.

4.1.3 Soil

The chemical composition profile for the soil source usually contains aluminium and silicon as major constituents along with lesser concentrations of Ca, Ti and Fe and other crustal matter elemental components in ratios typical of crustal matter minerals. However, as discussed in Section 3.1 it was found that the PTFE filters used in the Westport study had a high background of silicon that precluded obtaining any useful data for both Si and Al. However, using the data for Ca, Ti and Fe it was possible to extract an indication of the contribution of crustal matter to total particulate matter concentrations. The reduced data matrix places a greater uncertainty on the contribution as evidenced by the confidence intervals on the soil source contributions for $PM_{2.5}$ and PM_{10} as presented in Figures 3.4 and 3.5 respectively.

4.1.4 Marine Aerosol

Marine aerosol was found to be a significant contributor to $PM_{2.5}$ (17%) and a major contributor to PM_{10} (43%) in Westport and is generally a significant particle source in New Zealand airsheds due to the isolated oceanic location of the landmass. Figure 4.1 shows that marine aerosol contributions were highly correlated between the two size fractions as the generation of sea salt results in a primarily coarse particle size-range that extends down to $PM_{2.5}$.

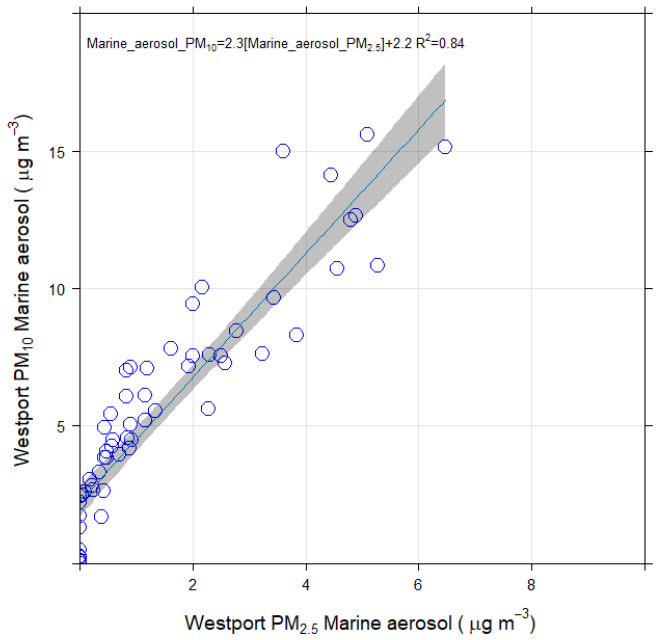

Figure 4.1 Marine aerosol contributions to $PM_{2.5}$ compared to PM_{10} for Westport.

The elemental composition for the marine aerosol source closely resembles that of seawater (Lide 1992), and the source profile is therefore dominated by chlorine and sodium. Analysis of peak marine aerosol contributions to PM concentrations (Figure 3.15) showed distinct northerly and southwest directionality during higher wind speeds at Westport, which was consistent with the most significant oceanic wind directions.

4.2 Analysis of Contributions to Particulate matter on Peak Days

For air quality management purposes and the protection of human health, contributions from the various sources to peak particulate matter concentration events are of most interest. Of

the days when samples were collected during the monitoring period, there were 6 days when $PM_{2.5}$ concentrations were higher than 15 µg m^{-3}, the WHO AAQG for $PM_{2.5}$. The relative source contributions to $PM_{2.5}$ on those peak days are presented in Figure 4.2.

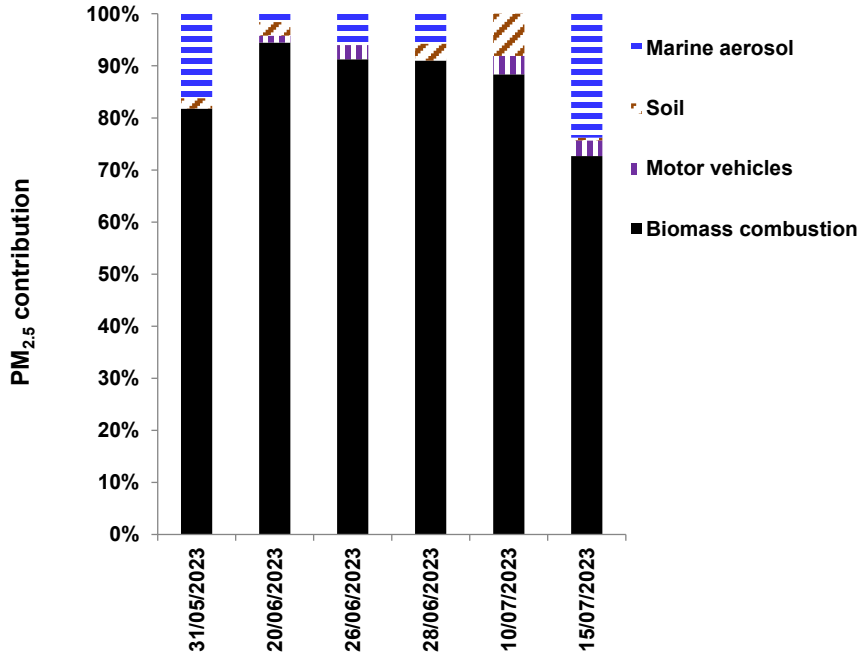

Figure 4.2 Source mass contributions to peak $PM_{2.5}$ events (> 15 µg m^{-3}) at Westport.

Figure 4.2 shows that biomass combustion was responsible for an average of 87% of $PM_{2.5}$ mass on high concentration days during winter. The result is consistent with the location of the Westport monitoring site in a residential area where solid fuel fires are used for home heating during winter. In New Zealand urban areas, high PM events are generally dominated by biomass burning emissions during winter. Concentrations generally peak in the late evening, and most (>90%) of the particulate matter is in the $PM_{2.5}$ fraction (Davy, Ancelet et al. 2012, Ancelet, Davy et al. 2014, Ancelet, Davy and Trompetter 2015, Davy, Ancelet and Trompetter 2016, Davy and Trompetter 2017, Davy and Trompetter 2019). During peak winter $PM_{2.5}$ concentrations, contributions from other emission sources were generally low, including any contribution from natural sources such as marine aerosol.

For PM_{10}, peak concentration days are considered to be concentrations above 33 µg m^{-3} (the 'Alert' category as described in Table 2.1). There was one sampling day during the monitoring campaign (on 1st of August 2023) where PM_{10} exceeded the Alert category. Interestingly, the data indicates that marine aerosol dominated PM_{10} source contributions on that day as shown in Figure 4.3. $PM_{2.5}$ was also high in marine aerosol for that sample (49%) while biomass combustion contributions were similar at 6.3 and 6.5 µg m^{-3} for $PM_{2.5}$ and PM_{10} respectively.

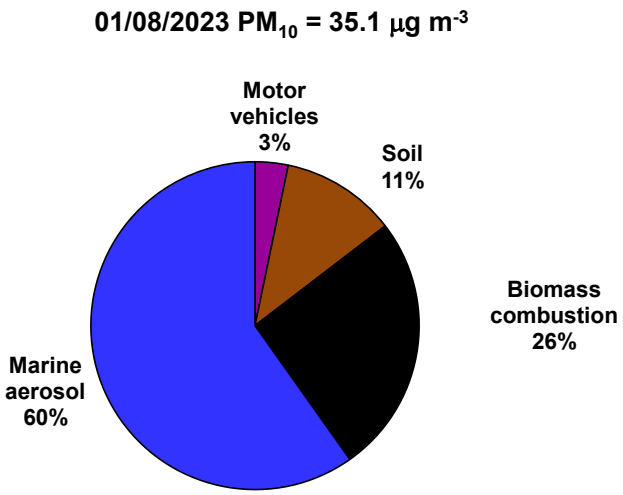

Figure 4.3 Source mass contributions to the peak PM_{10} event (> 33 µg m^{-3}) on 01/08/2023 at Westport.

5.0 SUMMARY OF WESTPORT PARTICULATE MATTER COMPOSITION AND SOURCE CONTRIBUTIONS

A winter (May 2023 to September 2023) $PM_{2.5}$ and PM_{10} airborne particle sampling programme at Westport formed the basis of a study of particulate matter composition and the attribution of sources contributing to particulate matter concentrations. The particulate matter elemental composition data showed that black carbon, a product from combustion sources, was a dominant contributor to $PM_{2.5}$ concentrations. For PM_{10}, black carbon, sodium and chlorine were also important components which indicate the primary influence of the $PM_{2.5}$ combustion sources along with coarse particle marine aerosol (sea salt) sources.

Four main source types were extracted from the data by receptor modelling techniques (using positive matrix factorisation), the sources of particulate matter were biomass combustion, motor vehicles, soil, and marine aerosol. The primary source of peak winter $PM_{2.5}$ in Westport was the biomass combustion source, which was attributed to the use of solid fuel fires for home heating and contributed 87% of the total $PM_{2.5}$ mass during peak concentrations (> than 15 µg m^{-3}). Contributions to peak PM_{10} concentrations reflected the influence of $PM_{2.5}$ combustion sources along with a greater influence of coarse particle sea salt and crustal matter. The biomass combustion source associated with home heating emissions was found to be contaminated with arsenic and lead due to the opportunistic use of copper chrome arsenate-treated timber and old painted timber, respectively, as fuel.

6.0 ACKNOWLEDGEMENTS

The authors thank Pam Rogers for the filter analytical measurements and Chris Purcell for XRF maintenance.

7.0 REFERENCES

Allen, J. O., P. R. Mayo, L. S. Hughes, L. G. Salmon and G. R. Cass (2001). "Emissions of size-segregated aerosols from on-road vehicles in the Caldecott tunnel." Environmental Science and Technology **35**(21): 4189-4197.

Ancelet, T. and P. Davy, K. (2015). Multi-elemental analysis of PM10 and apportionment of contributing sources during winter in Tokoroa, GNS Science Consultancy Report CR 2015/117 LR.

Ancelet, T., P. Davy, K., W. J. Trompetter, A. Markwitz and D. C. Weatherburn (2011). "Characterisation of particulate matter emissions from a modern wood burner under varying burner conditions." Air Quality and Climate Change **45**: 21-27.

Ancelet, T., P. K. Davy, T. Mitchell, W. J. Trompetter, A. Markwitz and D. C. Weatherburn (2012). "Identification of particulate matter sources on an hourly time-scale in a wood burning community." Environmental Science and Technology **46**(9): 4767-4774.

Ancelet, T., P. K. Davy and W. J. Trompetter (2013). Source apportionment of PM10 and PM2.5 in Nelson Airshed A. GNS Science consultancy report 2013/146, Institute of Geological and Nuclear Sciences**:** 95 p.

Ancelet, T., P. K. Davy and W. J. Trompetter (2014). Hourly concentrations of arsenic associated with Particulate Matter. 5th International Congress on Arsenic in the Environment, As 2014, Buenos Aires, CRC Press/Balkema.

Ancelet, T., P. K. Davy and W. J. Trompetter (2015). "Particulate matter sources and long-term trends in a small New Zealand city." Atmospheric Pollution Research **6**(6): 1105-1112.

Ancelet, T., P. K. Davy, W. J. Trompetter and A. Markwitz (2014). "Sources of particulate matter pollution in a small new zealand city." Atmospheric Pollution Research **5**(4): 572-580.

Ancelet, T., P. K. Davy, W. J. Trompetter, A. Markwitz and D. C. Weatherburn (2011). "Carbonaceous aerosols in an urban tunnel." Atmospheric Environment **45**(26): 4463-4469.

Ancelet, T., P. K. Davy, W. J. Trompetter, A. Markwitz and D. C. Weatherburn (2013). "Carbonaceous aerosols in a wood burning community in rural New Zealand." Atmospheric Pollution Research **4**(3): 245-249.

Ancelet, T., P. K. Davy, W. J. Trompetter, A. Markwitz and D. C. Weatherburn (2014). "Particulate matter sources on an hourly timescale in a rural community during the winter." Journal of the Air and Waste Management Association **64**(5): 501-508.

Ancelet, T., P. K. Davy, W. J. Trompetter, A. Markwitz and D. C. Weatherburn (2014). "Sources and transport of particulate matter on an hourly time-scale during the winter in a New Zealand urban valley." Urban Climate.

Anlauf, K., S.-M. Li, R. Leaitch, J. Brook, K. Hayden, D. Toom-Sauntry and A. Wiebe (2006). "Ionic composition and size characteristics of particles in the Lower Fraser Valley: Pacific 2001 field study." Atmospheric Environment **40**(15): 2662-2675.

Ashbaugh, L. L., W. C. Malm and W. Z. Sadeh (1985). "A residence time probability analysis of sulfur concentrations at Grand Canyon National Park." Atmos. Environ. **19**(8): 1263-1270.

Begum, B. A., P. K. Hopke and W. X. Zhao (2005). "Source identification of fine particles in Washington, DC, by expanded factor analysis modeling." Environ. Sci. Technol. **39**(4): 1129-1137.

Bennett, J., P. Davy, B. Trompetter, Y. Wang, N. Pierse, M. Boulic, R. Phipps and P. Howden-Chapman (2018). "Sources of indoor air pollution at a New Zealand urban primary school; a case study." Atmospheric Pollution Research.

Bond, T. C., S. J. Doherty, D. W. Fahey, P. M. Forster, T. Berntsen, B. J. DeAngelo, M. G. Flanner, S. Ghan, B. Kärcher, D. Koch, S. Kinne, Y. Kondo, P. K. Quinn, M. C. Sarofim, M. G. Schultz, M. Schulz, C. Venkataraman, H. Zhang, S. Zhang, N. Bellouin, S. K. Guttikunda, P. K. Hopke, M. Z. Jacobson, J. W. Kaiser, Z. Klimont, U. Lohmann, J. P. Schwarz, D. Shindell, T. Storelvmo, S. G. Warren and C. S. Zender (2013). "Bounding the role of black carbon in the climate system: A scientific assessment." Journal of Geophysical Research: Atmospheres **118**(11): 5380-5552.

Bond, T. C., D. G. Streets, K. F. Yarber, S. M. Nelson, J. H. Woo and Z. Klimont (2004). "A technology-based global inventory of black and organic carbon emissions from combustion." Journal of Geophysical Research D: Atmospheres **109**(14).

Brimblecombe, P. (1986). Air: Composition and Chemistry.

Brown, S. G., S. Eberly, P. Paatero and G. A. Norris (2015). "Methods for estimating uncertainty in PMF solutions: Examples with ambient air and water quality data and guidance on reporting PMF results." Science of the Total Environment **518-519**: 626-635.

Brown, S. G. and H. R. Hafner (2005). Multivariate Receptor Modelling Workbook. Research Triangle Park, NC, USEPA.

Cahill, T. A., R. A. Eldred, N. Motallebi and W. C. Malm (1989). "Indirect measurement of hydrocarbon aerosols across the United States by nonsulfate hydrogen-remaining gravimetric mass correlations." Aerosol Sci. Technol. **10**(2): 421-429.

Carslaw, D. C. (2012). The openair manual - open-source tools for analysing air pollution data. Manual for version 0.7-0, King's College London.

Carslaw, D. C. and K. Ropkins (2012). "openair - an R package for air quality data analysis." Environmental Modelling & Software **27-28**: 52-61.

Chueinta, W., P. K. Hopke and P. Paatero (2000). "Investigation of sources of atmospheric aerosol at urban and suburban residential areas in Thailand by positive matrix factorization." Atmos. Environ. **34**(20): 3319-3329.

Cohen, D., G. Taha, E. Stelcer, D. Garton and G. Box (2000). The measurement and sources of fine particle elemental carbon at several key sites in NSW over the past eight years. 15th Clean Air Conference, Sydney, Clean air Society of Australia and New Zealand.

Cohen, D. D. (1999). "Accelerator based ion beam techniques for trace element aerosol analysis." Advances in Environmental, Industrial and Process Control Technologies **1**(Elemental Analysis of Airborne Particles): 139-196.

Davy, P., K., T. Ancelet and W. J. Trompetter (2016). Source apportionment of PM2.5 and PM10-2.5 samples from St Albans, Christchurch, GNS Science Consultancy Report 2016/72.

Davy, P., K. and W. J. Trompetter (2017). Apportionment of PM2.5 and PM10 sources in the Richmond airshed, Tasman District. GNS Science Consultancy Report 2017/86

Institute of Geological and Nuclear Sciences**:** 69 p.

Davy, P., K. and W. J. Trompetter (2017). Apportionment of PM10 sources in the Tokoroa airshed, Waikato Region. GNS Science Consultancy Report 2017/75, Institute of Geological and Nuclear Sciences**:** 75 p.

Davy, P., K. and W. J. Trompetter (2018). Heavy metals, black carbon and natural sources of particulate matter in New Zealand. GNS Science consultancy report; 2017/238, Institute of Geological and Nuclear Sciences**:** 81 p.

Davy, P., K. and W. J. Trompetter (2019). Composition, sources and long-term trends for Auckland air particulate matter: Summary Report. GNS Science Consultancy Report 2019/151, Institute of Geological and Nuclear Sciences**:** 32 p.

Davy, P. K., T. Ancelet, W. J. Trompetter and A. Markwitz (2014). Arsenic and air pollution in New Zealand. 5th International Congress on Arsenic in the Environment, As 2014, Buenos Aires, CRC Press/Balkema.

Davy, P. K., T. Ancelet, W. J. Trompetter and A. Markwitz (2017). Source apportionment and trend analysis of air particulate matter in the Auckland region. GNS Science consultancy report 2014/194, Institute of Geological and Nuclear Sciences**:** 245 p.

Davy, P. K., T. Ancelet, W. J. Trompetter, A. Markwitz and D. C. Weatherburn (2012). "Composition and source contributions of air particulate matter pollution in a New Zealand suburban town." Atmospheric Pollution Research **3**(1): 143-147.

Davy, P. K., A. Markwitz and D. C. Weatherburn (2007). Composition, size and morphological comparison of wood smoke particles from source emissions and in urban air by SEM-EDS. Proc. 14th International Union of Air Pollution Prevention and Environmental Protection Associations (IUAPPA) World Congress 2007, 18th Clean Air Society of Australia and New Zealand (CASANZ) Conf., Brisbane, QLD.

Davy, P.K., Trompetter, W.J. 2023. Motueka: Composition and sources of PM2.5. Lower Hutt (NZ): GNS Science. 58 p. Consultancy Report 2023/77

Dirks, K. N., A. Chester, J. A. Salmond, N. Talbot, S. Thornley and P. Davy (2020). "Arsenic in hair as a marker of exposure to smoke from the burning of treated wood in domestic wood burners." International Journal of Environmental Research and Public Health **17**(11).

Dockery, D. W., H. Luttman-Gibson, D. Q. Rich, M. S. Link, M. A. Mittleman, D. R. Gold, P. Koutrakis, J. D. Schwartz and R. L. Verrier (2005). "Association of air pollution with increased incidence of ventricular tachyarrhythmias recorded by implanted cardioverter defibrillators." Environmental Health Perspectives **113**(6): 670-674.

Eberly, S. (2005). EPA PMF 1.1 User's Guide, USEPA.

Fine, P. M., G. R. Cass and B. R. Simoneit (2001). "Chemical characterization of fine particle emissions from fireplace combustion of woods grown in the northeastern United States." Environ. Sci. Technol. **35**(13): 2665-2675.

Fitzgerald, J. W. (1991). "Marine aerosols: A review." Atmospheric Environment - Part A General Topics **25**(3-4): 533-545.

Gard, E. E., M. J. Kleeman, D. S. Gross, L. S. Hughes, J. O. Allen, B. D. Morrical, D. P. Fergenson, T. Dienes, M. E. Galli, R. J. Johnson, G. R. Cass and K. A. Prather (1998). "Direct observation of heterogeneous chemistry in the atmosphere." Science (Washington, D. C.) **279**(5354): 1184-1187.

Geng, F., J. Hua, Z. Mu, L. Peng, X. Xu, R. Chen and H. Kan (2013). "Differentiating the associations of black carbon and fine particle with daily mortality in a Chinese city." Environmental Research **120**: 27-32.

George, I. J. and J. P. D. Abbatt (2010). "Heterogeneous oxidation of atmospheric aerosol particles by gas-phase radicals." Nature Chemistry **2**(9): 713-722.

Grange, S. K., J. A. Salmond, W. J. Trompetter, P. K. Davy and T. Ancelet (2013). "Effect of atmospheric stability on the impact of domestic wood combustion to air quality of a small urban township in winter." Atmospheric Environment **70**: 28-38.

Hays, M. D., S. H. Cho, R. Baldauf, J. J. Schauer and M. Shafer (2011). "Particle size distributions of metal and non-metal elements in an urban near-highway environment." Atmospheric Environment **45**(4): 925-934.

Hopke, P. K. (1999). "An introduction to source receptor modeling." Adv. Environ. Indust. Process Control Technol. **1**(Elemental Analysis of Airborne Particles): 273-315.

Hopke, P. K. (2003). "Recent developments in receptor modeling." J. Chemomet. **17**(5): 255-265.

Hopke, P. K., Y. L. Xie and P. Paatero (1999). "Mixed multiway analysis of airborne particle composition data." J. Chemomet. **13**(3-4): 343-352.

Horvath, H. (1993). "Atmospheric Light Absorption - A Review." Atmos. Environ, **27A**: 293-317.

Horvath, H. (1997). "Experimental calibration for aerosol light absorbtion measurements using the integrating plate method - Summary of the data." Aerosol Science **28**: 2885-2887.

Huang, X. F., J. Z. Yu, L. Y. He and M. Hu (2006). "Size distribution characteristics of elemental carbon emitted from Chinese vehicles: results of a tunnel study and atmospheric implications." Environmental Science and Technology **40**: 5355-5360.

Hung, N. T. Q., S. B. Lee, N. T. Hang, J. Kongpran, N. T. Kim Oanh, S. G. Shim and G. N. Bae (2014). "Characterization of black carbon at roadside sites and along vehicle roadways in the Bangkok Metropolitan Region." Atmospheric Environment **92**: 231-239.

Hyslop, N. P., K. Trzepla, S. Yatkin, W. H. White, T. Ancelet, P. Davy, O. Butler, M. Gerboles, S. Kohl, A. McWilliams, L. Saucedo, M. Van Der Haar and A. Jonkers (2019). "An inter-laboratory evaluation of new multi-element reference materials for atmospheric particulate matter measurements." Aerosol Science and Technology **53**(7): 771-782.

Jacobson, M. Z. (2001). "Strong radiative heating due to the mixing state of black carbon in atmospheric aerosols." Nature **409**(6821): 695-697.

Jeong, C.-H., P. K. Hopke, E. Kim and D.-W. Lee (2004). "The comparison between thermal-optical transmittance elemental carbon and Aethalometer black carbon measured at multiple monitoring sites." Atmos. Environ. **38**(31): 5193.

Kara, M., P. K. Hopke, Y. Dumanoglu, H. Altiok, T. Elbir, M. Odabasi and A. Bayram (2015). "Characterization of PM Using Multiple Site Data in a Heavily Industrialized Region of Turkey." Aerosol and Air Quality Research **15**(1): 11-+.

Ke, L., X. Ding, R. L. Tanner, J. J. Schauer and M. Zheng (2007). "Source contributions to carbonaceous aerosols in the Tennessee Valley Region." Atmospheric Environment **41**(39): 8898-8923.

Khalil, M. A. K. and R. A. Rasmussen (2003). "Tracers of wood smoke." Atmospheric Environment **37**(9-10): 1211-1222.

Kim, E., P. K. Hopke and E. S. Edgerton (2003). "Source identification of Atlanta aerosol by positive matrix factorization." J. Air Waste Manage. Assoc. **53**(6): 731-739.

Kim, E., P. K. Hopke, T. V. Larson, N. N. Maykut and J. Lewtas (2004). "Factor analysis of Seattle fine particles." Aerosol Sci. Technol. **38**(7): 724-738.

Kuschel, G., J. Metcalfe, S. Sridhar, P. Davy, K., K. Westport, K. Mason, T. Denne, J. Berentson-Shaw, S. Bell, S. Hales, J. Atkinson and A. Woodward (2022). Health and air pollution in New Zealand 2016 (HAPINZ 3.0): Volume 2 – Detailed methodology. Health and air pollution in New Zealand 2016 (HAPINZ 3.0). New Zealand, Ministry for the Environment, Ministry of Health, Te Manatū Waka Ministry of Transport, and Waka Kotahi NZ Transport Agency.

Lack, D. A., J. J. Corbett, T. Onasch, B. Lerner, P. Massoli, P. K. Quinn, T. S. Bates, D. S. Covert, D. Coffman, B. Sierau, S. Herndon, J. Allan, T. Baynard, E. Lovejoy, A. R. Ravishankara and E. Williams (2009). "Particulate emissions from commercial shipping: Chemical, physical, and optical properties." Journal of Geophysical Research D: Atmospheres **114**(4).

Lee, E., C. K. Chan and P. Paatero (1999). "Application of positive matrix factorization in source apportionment of particulate pollutants in Hong Kong." Atmos. Environ, **33**(19): 3201-3212.

Lee, J. H., Y. Yoshida, B. J. Turpin, P. K. Hopke, R. L. Poirot, P. J. Lioy and J. C. Oxley (2002). "Identification of sources contributing to Mid-Atlantic regional aerosol." J. Air Waste Manag. Assoc. **52**(10): 1186-1205.

Lide, D. R. (1992). CRC Handbook of Chemistry and Physics, CRC Press Inc.

Lopez-Reyes, A., G. Orozco-Rivera, K. Acuna-Askar, J. F. Villarreal-Chiu and J. M. Alfaro-Barbosa (2016). "Characterization of atmospheric black carbon in particulate matter over the Monterrey metropolitan area, Mexico, using scanning electron microscopy." Air Quality, Atmosphere and Health **9**(3): 223-229.

Malm, W. C., J. F. Sisler, D. Huffman, R. A. Eldred and T. A. Cahill (1994). "Spatial and seasonal trends in particle concentration and optical extinction in the United States." J. Geophys. Res. Atmos. **99**(D1): 1347-1370.

Mitchell, T., P. K. Davy, N. Kim, T. Ancelet and W. J. Trompetter (2013). Arsenic concentrations in a suburban New Zealand wood burning community. 21st Clean Air Society of Australia and New Zealand Conference, Sydney.

Norris, G., R. Duvall, S. Brown and S. Bai (2014). EPA Positive Matrix Factorization (PMF) 5.0 Fundamentals and User Guide. USEPA.

O'Dowd, C. D., J. A. Lowe, N. Clegg, M. H. Smith and S. L. Clegg (2000). "Modeling heterogeneous sulphate production in maritime stratiform clouds." J. Geophys. Res.- Atmos. **105**(D6): 7143-7160.

Paatero, P. (1997). "Least squares formulation of robust non-negative factor analysis." Chemom. Intell. Lab. Syst. **18**: 183-194.

Paatero, P. (2000). PMF User's Guide. Helsinki, University of Helsinki.

Paatero, P., S. Eberly, S. G. Brown and G. A. Norris (2014). "Methods for estimating uncertainty in factor analytic solutions." Atmos. Meas. Tech. **7**(3): 781-797.

Paatero, P. and P. K. Hopke (2002). "Utilizing wind direction and wind speed as independent variables in multilinear receptor modeling studies." Chemometrics and Intelligent Laboratory Systems **60**(1-2): 25-41.

Paatero, P. and P. K. Hopke (2003). "Discarding or downweighting high-noise variables in factor analytic models." Analytica Chimica Acta **490**(1-2): 277-289.

Paatero, P., P. K. Hopke, B. A. Begum and S. K. Biswas (2005). "A graphical diagnostic method for assessing the rotation in factor analytical models of atmospheric pollution." Atmospheric Environment **39**(1): 193-201.

Paatero, P., P. K. Hopke, X. H. Song and Z. Ramadan (2002). "Understanding and controlling rotations in factor analytic models." Chemometrics and Intelligent Laboratory Systems **60**(1-2): 253-264.

Patel, H., N. Talbot, J. Salmond, K. Dirks, S. Xie and P. Davy (2020). "Implications for air quality management of changes in air quality during lockdown in Auckland (New Zealand) in response to the 2020 SARS-CoV-2 epidemic." Science of The Total Environment **746**: 141129.

Posfai, M., A. Gelencser, R. Simonics, K. Arato, J. Li, P. V. Hobbs and P. R. Buseck (2004). "Atmospheric tar balls: Particles from biomass and biofuel burning." J. Geophys. Res. Atmos. **109**(D6).

Posfai, M., R. Simonics, J. Li, P. V. Hobbs and P. R. Buseck (2003). "Individual aerosol particles from biomass burning in southern Africa: 1. Compositions and size distributions of carbonaceous particles." J. Geophys. Res. Atmos. **108**(d13): 8483.

Ramadan, Z., B. Eickhout, X.-H. Song, L. M. C. Buydens and P. K. Hopke (2003). "Comparison of Positive Matrix Factorization and Multilinear Engine for the source apportionment of particulate pollutants." Chemomet. Intellig. Lab. Syst. **66**(1): 15-28.

Salako, G. O., P. K. Hopke, D. D. Cohen, B. A. Begum, S. K. Biswas, G. G. Pandit, Y. S. Chung, S. A. Rahman, M. S. Hamzah, P. Davy, A. Markwitz, D. Shagjjamba, S. Lodoysamba, W. Wimolwattanapun and S. Bunprapob (2012). "Exploring the variation between EC and BC in a variety of locations." Aerosol and Air Quality Research **12**(1): 1-7.

Schneider, J., U. Kirchner, S. Borrmann, R. Vogt and V. Scheer (2008). "In situ measurements of particle number concentration, chemically resolved size distributions and black carbon content of traffic-related emissions on German motorways, rural roads and in city traffic." Atmospheric Environment **42**(18): 4257-4268.

Scott, A. J. (2014). Timaru source apportionment study, Environment Canterbury Report No. R12/100.

Seinfeld, J. H. and S. N. Pandis (2006). Atmospheric Chemistry and Physics: From Air Pollution to Climate Change. New York, John Wiley & Sons, Inc.

Song, X. H., A. V. Polissar and P. K. Hopke (2001). "Sources of fine particle composition in the northeastern US." Atmospheric Environment **35**(31): 5277-5286.

Team, R. D. C. (2010). R: A language and environment for statistical computing. R Foundation for Statistical Computing, Vienna, Austria.

Trompetter, W. J. (2004). Ion Beam Analysis results of air particulate filters from the Wellington Regional Council. Wellington, Geological and Nuclear Sciences Limited.

Trompetter, W. J., P. K. Davy and A. Markwitz (2010). "Influence of environmental conditions on carbonaceous particle concentrations within New Zealand." Journal of Aerosol Science **41**(1): 134-142.

Trompetter, W. J., S. K. Grange, P. K. Davy and T. Ancelet (2013). "Vertical and temporal variations of black carbon in New Zealand urban areas during winter." Atmospheric Environment **75**: 179-187.

Watson, J. G., J. C. Chow and C. A. Frazier (1999). "X-ray fluorescence analysis of ambient air samples." Adv. Environ., Ind. Process Control Technol. **1**(Elemental Analysis of Airborne Particles): 67-96.

Wilton, E., J. Smith and P. Davy (2007). Source identification and apportionment of PM10 and PM2.5 in Westport and Auckland, NIWA.

Yatkin, S., K. Trzepla, N. P. Hyslop, W. H. White, O. Butler, T. Ancelet, P. Davy, M. Gerboles, S. D. Kohl, A. McWilliams, L. Saucedo, M. Van Der Haar and A. Jonkers (2020). "Comparison of a priori and interlaboratory-measurement-consensus approaches for value assignment of multi-element reference materials on PTFE filters." Microchemical Journal **158**.

Zanobetti, A. and J. Schwartz (2006). "Air pollution and emergency admissions in Boston, MA." Journal of Epidemiology and Community Health **60**(10): 890-895.

This page left intentionally blank.

APPENDICES

This page left intentionally blank.

APPENDIX 1 ANALYSIS TECHNIQUES

A1.1 X-ray Fluorescence Spectroscopy (XRF)

X-ray fluorescence spectroscopy (XRF) was used to measure elemental concentrations in $PM_{2.5}$ and PM_{10} samples collected on PTFE filters at Westport. XRF measurements in this study were carried out at the GNS Science XRF facility, and the spectrometer used was a PANalytical Epsilon 5 (PANalytical, the Netherlands). The Epsilon 5 is shown in Figure A1.1. XRF is a non-destructive and relatively rapid method for the elemental analysis of particulate matter samples.

Figure A1.1 The PANalytical Epsilon 5 spectrometer.

XRF is based on the measurement of characteristic X-rays produced by the ejection of an inner shell electron from an atom in the sample, creating a vacancy in the inner atomic shell. A higher energy electron then drops into the lower energy orbital and releases a fluorescent X-ray to remove excess energy (Watson, Chow and Frazier 1999). The energy of the released X-ray is characteristic of the emitting element, and the area of the fluorescent X-ray peak (intensity of the peak) is proportional to the number of emitting atoms in the sample. From the intensity, it is possible to calculate a specific element's concentration by direct comparison with standards.

To eject inner shell electrons from atoms in a sample, the XRF spectrometer at GNS Science uses a 100 kV Sc/W X-ray tube. The 100 kV X-rays produced by this tube are able to provide elemental information for elements from Na–U. Unlike ion beam analysis techniques, which are similar to XRF, the PANalytical Epsilon 5 is able to use characteristic K-lines produced by each element for quantification. This is crucial for optimising limits of detection because K-lines have higher intensities and are located in less crowded regions of the X-ray spectrum. The X-

rays emitted by the sample are detected using a high-performance Ge detector, which further improves the detection limits. Figure A1.2 presents a sample X-ray spectrum.

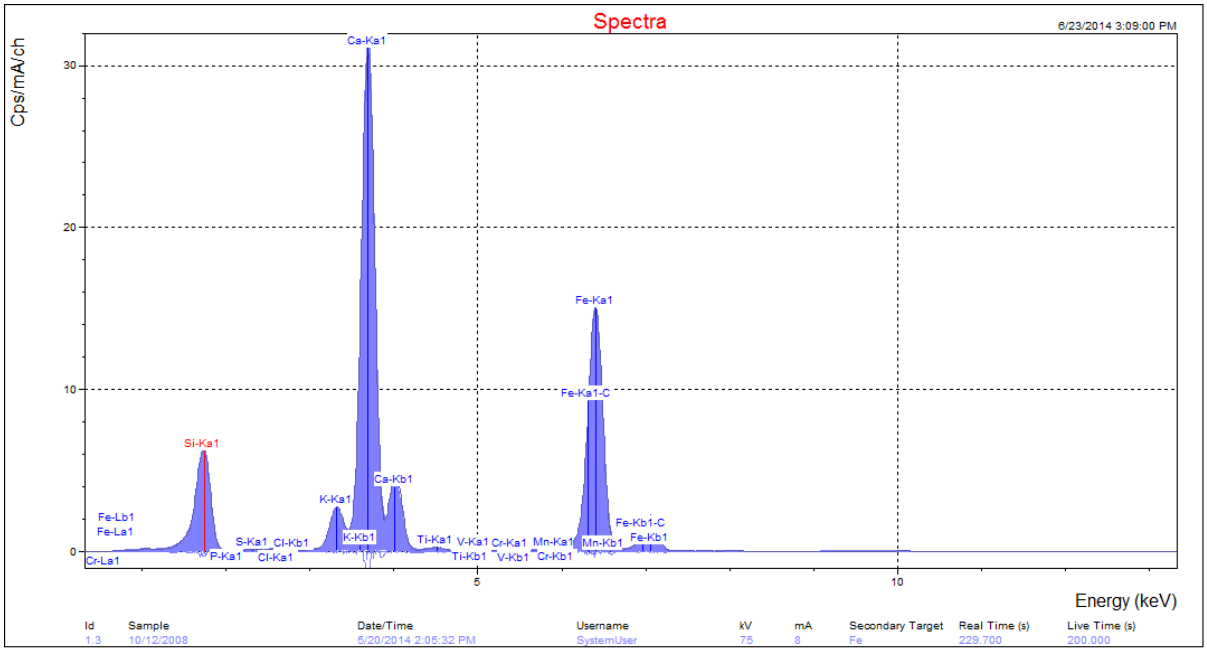

Figure A1.2 Example X-ray spectrum from a PM_{10} sample.

In this study, calibration standards for each of the elements of interest were analysed prior to the samples being run. Once the calibration standards were analysed, spectral deconvolutions were performed using PANalytical software to correct for line overlaps and ensure that the spectra were accurately fit. Calibration curves for each element of interest were produced and used to determine the elemental concentrations from the Westport samples. Multi-elemental reference standards were also analysed to ensure that the results obtained were robust and accurate (Hyslop, Trzepla et al. 2019, Yatkin, Trzepla et al. 2020).

A1.2 Black carbon measurements

Black carbon (BC) is a combustion-derived atmospheric aerosol that has important implications for human health and the Earth's climate. Exposure to ambient concentrations of BC has been associated with significant negative impacts on human health, including increased hospital admissions and mortality due to cardiovascular diseases (Dockery, Luttman-Gibson et al. 2005, Zanobetti and Schwartz 2006, Geng, Hua et al. 2013). Black carbon also plays a unique role in the Earth's climate system. While most aerosols in the atmosphere scatter incoming solar radiation, resulting in a net cooling effect on the atmosphere, BC absorbs significantly more light than it reflects, resulting in a net warming effect. Light absorbing particles radiate long-wave energy that heats the surrounding air. This results in a positive (warming) forcing (Jacobson 2001). The magnitude of BC's warming has recently been estimated to be the 2nd highest warming species, trailing only the effects of carbon dioxide (Bond, Doherty et al. 2013). Research regarding the concentrations and effects of BC is ongoing, and, as more research is undertaken, it is likely that these and other effects will be further quantified.

Black carbon particle size ranges have been well characterised over a variety of emission sources, both in New Zealand (Davy, Markwitz and Weatherburn 2007, Ancelet, Davy et al. 2011, Ancelet, Davy et al. 2011, Davy, Ancelet et al. 2012, Salako, Hopke et al. 2012, Ancelet,

Davy et al. 2013, Trompetter, Grange et al. 2013) and internationally (Ke, Ding et al. 2007, Schneider, Kirchner et al. 2008, Lack, Corbett et al. 2009, Hays, Cho et al. 2011, Lopez-Reyes, Orozco-Rivera et al. 2016) and are invariably found to be in the sub-micrometre size range. Black carbon particles can consist of individual spherules (10-30 nm in diameter) to larger agglomerations (300 – 500 nm diameter) of individual particles. Black carbon (often called "soot") is usually formed under conditions in which insufficient oxygen is present for complete oxidation of carbonaceous fuel to CO_2 (fuel-rich) (Bond, Streets et al. 2004). The characteristics of the combustion source therefore have an important bearing on particle size and carbonaceous composition with high temperature combustion conditions (diesel engines, power stations) producing smaller, graphitic carbon particle entities (Allen, Mayo et al. 2001, Huang, Yu et al. 2006, Ancelet, Davy et al. 2011, Hung, Lee et al. 2014) whereas lower temperature biomass combustion (wood fires for home heating, wild fire, forest fires) produce a mixture of carbon agglomerations and larger particles (500 – 900 nm) composed of a soot core and coated in organic 'tar' from incomplete combustion (Posfai, Simonics et al. 2003, Posfai, Gelencser et al. 2004, Davy, Markwitz and Weatherburn 2007).

Determination of carbon (soot) on filters was performed by light reflection to provide the BC concentration. The absorption and reflection of visible light on particles in the atmosphere or collected on filters is dependent on the particle concentration, density, refractive index and size. For atmospheric particles, BC is the most highly absorbing component in the visible light spectrum with very much smaller components coming from soils, sulphates and nitrate (Horvath 1993, Horvath 1997). Hence, to the first order it can be assumed that all the absorption on atmospheric filters is due to BC. The main sources of atmospheric BC are anthropogenic combustion sources and include biomass burning, motor vehicles and industrial emissions (Cohen, Taha et al. 2000). Cohen and co-workers found that BC is typically 10 – 40 % of the fine mass ($PM_{2.5}$) fraction in many urban areas of Australia.

When measuring BC by light reflection/transmission, light from a light source is transmitted through a filter onto a photocell. The amount of light absorption is proportional to the amount of black carbon present and provides a value that is a measure of the black carbon on the filter. Conversion of the absorbance value to an atmospheric concentration value of BC requires the use of an empirically derived equation (Cohen, Taha et al. 2000):

$$BC\ (\mu g\ cm^{-2}) = (100/2(F\varepsilon))\ \ln[R_0/R] \qquad \text{Equation A1.1}$$

where:

ε is the mass absorbent coefficient for BC ($m^2\ g^{-1}$) at a given wavelength;

F is a correction factor to account for other absorbing factors such as sulphates, nitrates, shadowing and filter loading. These effects are generally assumed to be negligible, and F is set at 1.00;

R_0, R are the pre- and post-reflection intensity measurements, respectively.

Black carbon was measured at GNS Science using the M43D Digital Smoke Stain Reflectometer. The following equation (from Willy Maenhaut, Institute for Nuclear Sciences, University of Gent Proeftuinstraat 86, B-9000 GENT, Belgium) was used for obtaining BC from reflectance measurements on Nucleopore polycarbonate filters or Pall Life Sciences Teflon filters:

$$BC\ (\mu g\ cm^{-2}) = [1000 \times LOG(R_{blank}/R_{sample}) + 2.39] / 45.8 \qquad \text{Equation A1.2}$$

where:

R_{blank}: the average reflectance for a series of blank filters; R_{blank} is close (but not identical) to 100. GNS always use the same blank filter for adjusting to 100.

R_{sample}: the reflectance for a filter sample (normally lower than 100).

With: 2.39 and 45.8 constants derived using a series of 100 Nuclepore polycarbonate filter samples which served as secondary standards; the BC loading (in μg cm^{-2}) for these samples had been determined by Prof. Dr. M.O. Andreae (Max Planck Institute of Chemistry, Mainz, Germany) relative to standards that were prepared by collecting burning acetylene soot on filters and determining the mass concentration gravimetrically (Trompetter 2004).

A1.3 Positive Matrix Factorization

Positive matrix factorisation (PMF) is a linear least-squares approach to factor analysis and was designed to overcome the receptor modeling problems associated with techniques like principal components analysis (PCA) and the *a priori* knowledge required for chemical mass balance approaches (Paatero, Hopke et al. 2005). With PMF, sources are constrained to have non-negative species concentrations, no sample can have a negative source contribution, and error estimates for each observed data point are used as point-by-point weights. This feature is a distinct advantage, in that it can accommodate missing and below detection limit data that is a common feature of environmental monitoring results (Song, Polissar and Hopke 2001). In fact, the signal to noise ratio for an individual elemental measurement can have a significant influence on a receptor model and modeling results. For the weakest (closest to detection limit) species, the variance may be entirely from noise (Paatero and Hopke 2002). Paatero and Hopke (2002) strongly suggest down-weighting or discarding noisy variables that are always below their detection limit or species that have a lot of error in their measurements relative to the magnitude of their concentrations (Paatero and Hopke 2003). The distinct advantage of PMF is that mass concentrations can be included in the model and the results are directly interpretable as mass contributions from each factor (source).

A1.4 PMF model outline

The mathematical basis for PMF is described in detail by Paatero (Paatero 1997, Paatero 2000). Briefly, PMF uses a weighted least-squares fit with the known error estimates of measured elemental concentrations used to derive the weights. In matrix notation, this is indicated as:

$$X = GF + E \qquad \text{Equation A1.3}$$

where:

X is the known n x m matrix of m measured elemental species in n samples;

G is an n x p matrix of source contributions to the samples;

F is a p x m matrix of source compositions (source profiles).

E is a residual matrix – the difference between measurement X and model Y.

E can be defined as a function of factors G and F:

$$e_{ij} = x_{ij} - y_{ij} = x_{ij} - \sum_{k=1}^{p} g_{ik} f_{kj}$$

Equation A1.4

where:

i = 1,……,*n* elements

j = 1,……,*m* samples

k = 1,…...,*p* sources

PMF constrains all elements of *G* and *F* to be non-negative, meaning that elements cannot have negative concentrations and samples cannot have negative source contributions as in real space. The task of PMF is to minimise the function *Q* such that:

$$Q(E) = \sum_{i=1}^{n} \sum_{j=1}^{m} (e_{ik} / \sigma_{kj})^2$$

Equation A1.5

where σ_{kj} is the error estimate for x_{ij}. Another advantage of PMF is the ability to handle extreme values typical of air pollutant concentrations as well as true outliers that would normally skew PCA. In either case, such high values would have significant influence on the solution (commonly referred to as leverage). PMF has been successfully applied to receptor modeling studies in a number of countries around the world (Hopke, Xie and Paatero 1999, Lee, Chan and Paatero 1999, Chueinta, Hopke and Paatero 2000, Song, Polissar and Hopke 2001, Lee, Yoshida et al. 2002, Kim, Hopke and Edgerton 2003, Jeong, Hopke et al. 2004, Kim, Hopke et al. 2004, Begum, Hopke and Zhao 2005) including New Zealand (Ancelet, Davy et al. 2012, Davy, Ancelet et al. 2012, Ancelet, Davy et al. 2014, Bennett, Davy et al. 2018, Davy and Trompetter 2019, Patel, Talbot et al. 2020).

A1.4.1 PMF model used

Two programs have been written to implement different algorithms for solving the least squares PMF problem, these are PMF2 and EPAPMF, the latter incorporates the Multilinear Engine (ME-2) (Hopke, Xie and Paatero 1999, Ramadan, Eickhout et al. 2003). In effect, the EPAPMF program provides a more flexible framework than PMF2 for controlling the solutions of the factor analysis with the ability of imposing explicit external constraints.

This study used EPAPMF 5.0 (version 14.0), which incorporates a graphical user interface (GUI) based on the ME-2 program. Both PMF2 and EPAPMF programs can be operated in a robust mode, meaning that “outliers” are not allowed to overly influence the fitting of the contributions and profiles (Eberly 2005). The user specifies two input files, one file with the concentrations and one with the uncertainties associated with those concentrations. The methodology for developing an uncertainty matrix associated with the elemental concentrations for this work is discussed in Section A1.4.2.

A1.4.2 PMF model inputs

The PMF programs provide the user with a number of choices in model parameters that can influence the final solution. Two parameters, the 'signal-to-noise ratio' and the 'species category' are of particular importance and are described below.

Signal-to-noise ratio (S/N) - this is a useful diagnostic statistic estimated from the input data and uncertainty files. Two calculations are performed to determine S/N, where concentrations below uncertainty are determined to have no signal, and for concentrations above uncertainty, the difference between concentration (x_i) and uncertainty (s_i) is used as the signal.

$$d_{ij} = \left(\frac{x_{ij} - s_{ij}}{s_{ij}} \right) \quad \text{if } x_{ij} > s_{ij}$$

$$d_{ij} = 0 \qquad \text{if } x_{ij} \leq s_{ij}$$

S/N is then calculated using Equation A1.6:

$$\left(\frac{S}{N} \right)_j = 1/n \sum_{i=1}^{n} d_{ij}$$

Equation A1.6

The result with this S/N calculation is that species with concentrations always below their uncertainty have a S/N of 0. Species with concentrations that are twice the uncertainty value have a S/N of 1. S/N greater than 1 may often indicate a species with a "good" signal, though this depends on how uncertainties were determined. Negative concentration values do not contribute to the S/N, and species with a handful of high concentration events will not have artificially high S/N (Norris, Duvall et al. 2014).

Species category – this enables the user to specify whether the elemental species should be considered:

- Strong – whereby the element is generally present in concentrations well above the LOD (high signal to noise ratio) and the uncertainty matrix is a reasonable representation of the errors.
- Weak – where the element may be present in concentrations near the LOD (low signal to noise ratio); there is doubt about some of the measurements and/or the error estimates; or the elemental species is only detected some of the time. If 'Weak' is chosen EPAPMF increases the user-provided uncertainties for that variable by a factor of 3.
- Bad – that variable is excluded from the model run.

For this work, an element with concentrations at least 3 times above the LOD, a high signal to noise ratio (> 2) and present in all samples was generally considered 'Strong'. Variables were labelled as 'Weak' if their concentrations were generally low, had a low signal to noise ratio, were only present in a few samples or there was a lower level of confidence in their measurement. Mass concentration gravimetric measurements and BC were also down weighted as 'Weak' depending on the dataset because their concentrations are generally several orders of magnitude above other species, which can have the tendency to 'pull' the

model. Paatero and Hopke recommend that such variables be down-weighted and that it doesn't particularly affect the model fitting if those variables are from real sources (Paatero and Hopke 2003). What does affect the model severely is if a dubious variable is over-weighted. Elements that had a low signal to noise ratio (< 0.5) were examined using bivariate correlation plots to determine interspecies relationships. Those low S/N variables with little or no association with other species, or had mostly zero values, or were doubtful for any reason, were labelled as 'Bad' and were subsequently not included in the analyses.

If the model is appropriate for the data and if the uncertainties specified are truly reflective of the uncertainties in the data, then *Q* (according to Eberly) should be approximately equal to the number of data points in the concentration data set (Eberly 2005):

*Theoretical Q = # samples **x** # species measured* Equation A1.7

However, a slightly different approach to calculating the Theoretical *Q* value was recommended by Brown and Hafner (2005), which takes into account the degrees of freedom in the PMF model and the additional constraints in place for each model run. This theoretical *Q* calculation Q_{th} is given as:

$$Q_{th} = (\#\ samples \times \#\ good\ species) + [(\#\ samples \times \#\ weak\ species)/3] - (\#\ samples \times factors\ estimated)$$ Equation A1.8

Both approaches have been taken into account for this study and it is likely that the actual value lies somewhere between the two. Further guidance has more recently been provided by Paatero and co-workers (Paatero, Eberly et al. 2014, Brown, Eberly et al. 2015) where a third parameter, $Q_{expected}$ should also be calculated, but only the "good" or non-weak variables should be taken into account:

The expected value of Q is approximately = (number of non-weak data values in X) − (numbers of elements in G and F, taken together). Equation A1.9

A downweighted weak variable has only a small, rarely significant contribution to $Q_{expected}$, and for simplicity is excluded here. If the Q value of the chosen model differs significantly from what is expected (e.g., by a factor of ten or more), then DISP error analysis becomes invalid and BS-DISP is likely questionable.

In PMF, it is assumed that only the x_{ij}'s are known and that the goal is to estimate the contributions (g_{ik}) and the factors (or profiles) (f_{kj}). It is assumed that the contributions and mass fractions are all non-negative, hence the "constrained" part of the least-squares. Additionally, EPAPMF allows the user to say how much uncertainty there is in each x_{ij}. Species-days with lots of uncertainty are not allowed to influence the estimation of the contributions and profiles as much as those with small uncertainty, hence the "weighted" part of the least squares and the advantage of this approach over PCA.

Diagnostic outputs from the PMF models were used to guide the appropriateness of the number of factors generated and how well the receptor modelling was accounting for the input data. Where necessary, initial solutions have been 'rotated' to provide a better separation of factors (sources) that were considered physically reasonable (Paatero, Hopke et al. 2002). Each PMF model run reported in this study is accompanied by the modelling statistics along with comments where appropriate.

A1.5 Dataset quality assurance

Quality assurance of sample elemental datasets is vital so that any dubious samples, measurements and outliers are removed as these will invariably affect the results of receptor modelling. In general, the larger the dataset used for receptor modelling, the more robust the analysis. The following sections describe the methodology used to check data integrity and provide a quality assurance process that ensured that the data being used in subsequent factor analysis was as robust as possible.

A1.5.1 Mass reconstruction and mass closure

Once the sample analysis for the range of analytes has been carried out, it is important to check that total measured mass does not exceed gravimetric mass (Cohen 1999). Ideally, when elemental analysis and organic compound analysis has been undertaken on the same sample, one can reconstruct the mass using the following general equation for ambient samples as a first approximation (Cahill, Eldred et al. 1989, Malm, Sisler et al. 1994, Cohen 1999):

Reconstructed mass = [Soil] + [OC] + [BC] + [Smoke] + [Sulphate] + [Sea salt] Equation A1.10

where:

[Soil] = 2.20[Al] + 2.49[Si] + 1.63[Ca] + 2.42[Fe] + 1.94[Ti]

[OC] = Σ[Concentrations of organic compounds]

[BC] = Concentration of black carbon (soot)

[Smoke] = [K] − 0.6[Fe]

[Sea salt] = 2.54[Na]

[Sulphate] = 4.125[S]

The reconstructed mass (RCM) is based on the fact that the six composite variables or ‘pseudo’ sources given in Equation A1.10 are generally the major contributors to fine and coarse particle mass and are based on geochemical principles and constraints. The [Soil] factor contains elements predominantly found crustal matter (Al, Si, Ca, Fe, Ti) and includes a multiplier to correct for oxygen content and an additional multiplier of 1.16 to correct for the fact that three major oxide contributors (MgO, K_2O, Na_2O) carbonate and bound water are excluded from the equation.

[BC] is the concentration of black carbon, measured in this case by light reflectance/absorbance. [Smoke] represents K not included as part of crustal matter and tends to be an indicator of biomass burning.

[Sea salt] represents the marine aerosol contribution and assumes that the NaCl weight is 2.54 times the Na concentration. Na is used as it is well known that Cl can be volatilised from aerosol or from filters in the presence of acidic aerosol, particularly in the fine fraction via the following reactions (Lee, Chan and Paatero 1999):

$$NaCl(p) + HNO_3(ag) \rightarrow NaNO_3(p) + HCL(g)$$ Equation A1.11

$$2NaCl(p) + H_2SO_4(ag) \rightarrow Na_2SO_4(p) + 2HCL(g)$$ Equation A1.12

Alternatively, where Cl loss is likely to be minimal, such as in the coarse fraction or for both size fractions near coastal locations and relatively clean air in the absence of acid aerosol, then the reciprocal calculation of [Sea salt] = 1.65[Cl] can be substituted, particularly where Na concentrations are uncertain.

Most fine sulphate particles are the result of oxidation of SO_2 gas to sulphate particles in the atmosphere (Malm, Sisler et al. 1994). It is assumed that sulphate is present in fully neutralised form as ammonium sulphate. [Sulphate] therefore represents the ammonium sulphate contribution to aerosol mass with the multiplicative factor of 4.125[S] to account for ammonium ion and oxygen mass (i.e., $(NH_4)_2SO_4$ = ((14 + 4)2 + 32 + (16x4)/32)).

Additionally, the sulphate component not associated with sea salt can be calculated from equation A1.14 (Cohen 1999):

$$\text{Non-sea salt sulphate (NSS-Sulphate)} = 4.125\ ([S_{tot}] - 0.0543[Cl]) \qquad \text{Equation A1.13}$$

Where the sulphur concentrations contributed by sea salt are inferred from the chlorine concentrations, i.e., [S/Cl] sea salt = 0.0543 and the factor of 4.125 assumes that the sulphate has been fully neutralised and is generally present as $(NH_4)_2SO_4$ (Cahill, Eldred *et al*. 1990; Malm, Sisler *et al*. 1994; Cohen 1999).

The RCM and mass closure calculations using the pseudo-source and pseudo-element approach are a useful way to examine initial relationships in the data and how the measured mass of species in samples compares to gravimetric mass. Note that some scatter is possible because not all aerosols are necessarily measured and accounted for, such as all OC, ammonium species, nitrates and unbound water.

A1.5.2 Dataset preparation

Careful preparation of a dataset is required because serious errors in data analysis and receptor modeling results can be caused by erroneous individual data values. The general methodology followed for dataset preparation was as recommended by Brown and Hafner (2005) and the EPAPMF 5.0 User Guide (Norris, Duvall et al. 2014). For this study, all data were checked for consistency with the following parameters:

- Individual sample collection validation;
- Gravimetric mass validation;
- Analysis of RCM versus gravimetric mass to assess mass closure and linearity;
- Identification of unusual values including noticeably extreme values and values that normally track with other species (e.g., Al and Si) but deviate in one or two samples. Scatter plots and time series plots were used to identify unusual values. One-off events such as fireworks displays, forest fires or vegetative burn-offs may affect a receptor model as it is forced to find a profile that matches only that day;
- Species were included in a dataset if at least 70% of data was above the LOD, and signal-to-noise ratios were checked to ensure data had sufficient variability. Important tracers of a source where less than 70% of data was above the LOD were included but model runs with and without the data were used to assess the effect;

In practice, during data analyses, the above steps were a reiterative process of cross checking as issues were identified and corrected for, or certain data excluded, and the effects of this were then studied.

A1.5.2.1 PMF data matrix population

The following steps were followed to produce a final dataset for use in the PMF receptor model (Brown and Hafner 2005).

Below detection limit data: For given values, the reported concentration used and the corresponding uncertainty checked to ensure it had a high value.

Missing data: Substituted with the dataset median value for that species.

A1.5.2.2 PMF uncertainty matrix population

Uncertainties can have a large effect on model results so that they must be carefully compiled. The effect of underestimating uncertainties can be severe, while overestimating uncertainties does not do too much harm (Paatero and Hopke 2003).

Uncertainties for data: Uncertainties for the XRF elemental data were calculated using the following equations (Kara, Hopke et al. 2015):

$\sigma_{ij} = x_{ij} + 2/3(DL_j)$ for samples below limit of detection;

$\sigma_{ij} = 0.2x_{ij} + 2/3(DLj)$; $DL_j < x_{ij} < 3DL_j$ and $\sigma_{ij} = 0.1x_{ij} + 2/3(DL_j)$; $x_{ij} > 3DL_j$: for detected values

where x_{ij} is the determined concentration for species j in the ith sample, and DL_j is the detection limit for species j.

Missing data: Uncertainty was calculated as 4 × median value over the entire species dataset.

PM gravimetric mass: Uncertainty given as 4 × mass value to down-weight the variable.

Reiterative model runs were used to examine the effect of including species with high uncertainties or low concentrations. In general, it was found that the initial uncertainty estimations were sufficient and that adjusting the ‘additional modelling uncertainty’ function accommodated any issues with modelled variables such as those with residuals outside ± 3 standard deviations.

APPENDIX 2 WESTPORT 2023 PM DATA ANALYSIS SUMMARY

Using the methodology outlined in Section A1.4.1, Figure A2.1, presents the mass reconstruction results for Westport $PM_{2.5}$ and PM_{10}. Figure A2.2 presents a correlation matrix plot for key elemental species in the two size fractions.

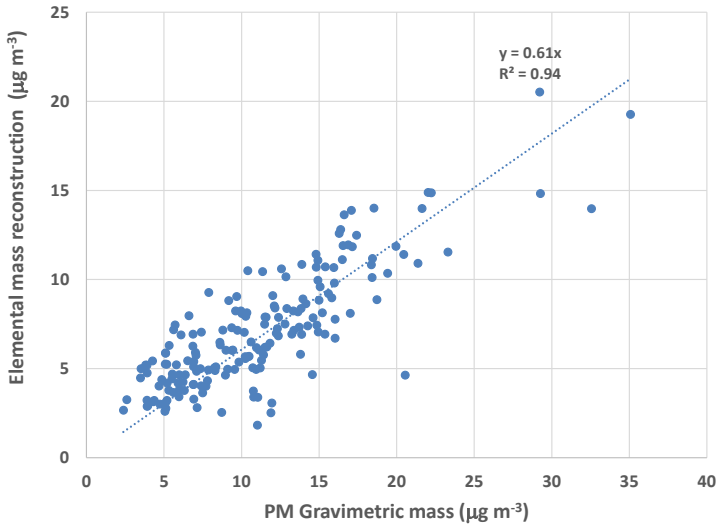

Figure A2.1 Plot of Westport $PM_{2.5}$ and PM_{10} elemental mass reconstruction against gravimetric mass.

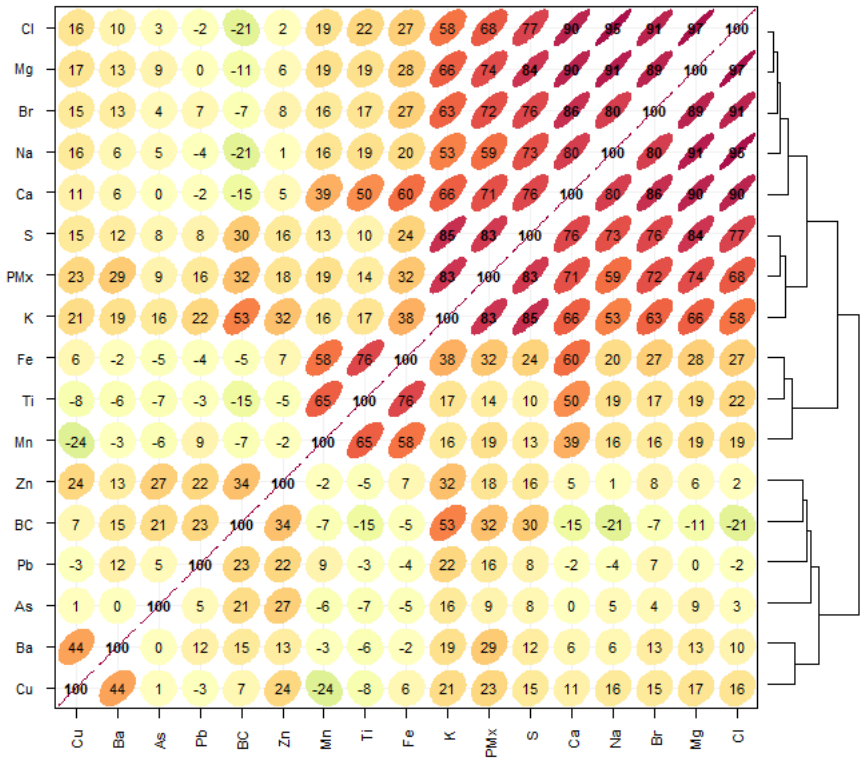

Figure A2.2 Particulate matter and key elemental composition correlation plot for Westport $PM_{2.5}$ and PM_{10} samples.

A2.1 WESTPORT PMF RECEPTOR MODELLING DIAGNOSTICS

PMF analyses involve many details about the development of the data, decisions of what data to include/exclude, determination of a solution, and evaluation of robustness of that solution. The following diagnostics for the PMF solutions are reported as recommended by Paatero and co-workers (Paatero, Eberly et al. 2014, Brown, Eberly et al. 2015) and should be read in conjunction with Section 2.1 and Appendix 1. A critical factor in the success of receptor modelling is the ability to reproduce observed versus predicted (modelled) mass. This was achieved to an acceptable level the in case of Westport $PM_{2.5}$ and PM_{10} as presented in Figure A2.3.

Summary of EPA PMF settings for receptor modelling of Westport $PM_{2.5}$ and PM_{10}

Parameter	Setting
Data type; averaging timeframe	$PM_{2.5}$ 24-hour
N samples	103
N factors	4
Treatment of missing data	No missing data
Treatment of data below detection limit (BDL)	Data used as reported, no modification or censoring of BDL data
Lower limit for normalised factor contributions gik	-0.2
Robust mode	Yes
Constraints	None
Seed value	Random
N bootstraps in BS	200
r^2 for BS	0.6
DISP dQmax	4, 8, 16, 32
DISP active species	PM2.5, BC, Na, Mg, S, Cl, K, Ca, Ti, Fe, Cu
N bootstraps; r^2 for BS in BS-DISP	200; 0.6
BS-DISP active species	BC, Na, Mg, S, Cl, K, Ca, Ti, Fe, Cu
BS-DISP dQmax	0.5, 1, 2, 4
Extra modelling uncertainty	15%

Output diagnostics for receptor modelling of Westport $PM_{2.5}$ and PM_{10}

Diagnostic	4 factors
$Q_{Theoretical}$	1550
$Q_{Expected}$	1258
Q_{true}	859
Q_{robust}	859
$Q_{robust}/Q_{expected}$	0.707
DISP Diagnostics	
Error code	0
Largest Decrease in Q:	0
DISP % dQ	0
DISP swaps by factor	0
BS-DISP Diagnostics	
BS mapping (Fpeak BS) - Unmapped	88% (98%) - 6
BS-DISP % cases accepted	66%
Largest Decrease in Q:	-26.3
BS-DISP % dQ	-3.06
# of Decreases in Q:	9
# of Swaps in Best Fit:	54
# of Swaps in DISP:	25
BS-DISP swaps by factor	4,57,1,58

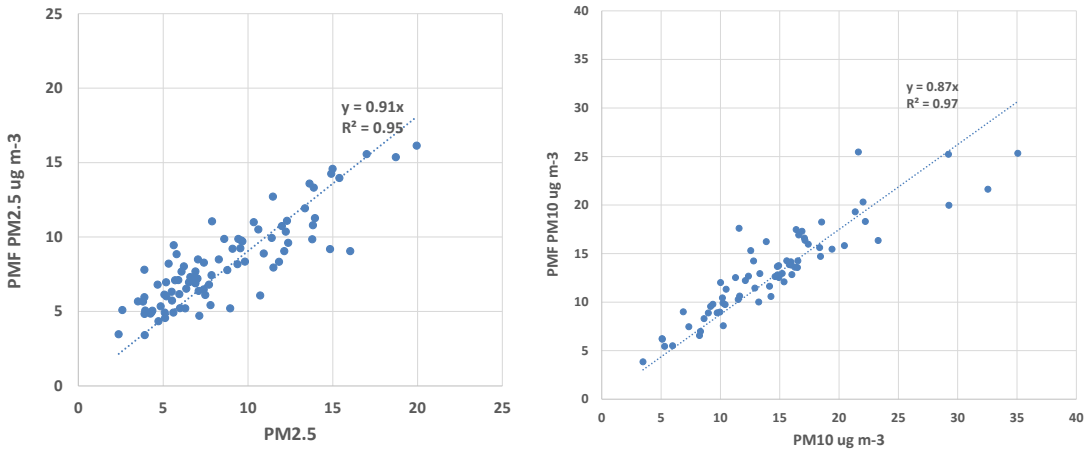

Figure A2.3 Plot of Westport $PM_{2.5}$ (left) and PM_{10} (right) predicted (PMF mass) against observed gravimetric mass.